Molecular Therapy
Nucleic Acids
Original Article

Long Non-coding RNA Profiling Reveals an Abundant MDNCR that Promotes Differentiation of Myoblasts by Sponging miR-133a

Hui Li,[1,4] Jiameng Yang,[1,4] Rui Jiang,[1] Xuefeng Wei,[2] Chengchuang Song,[1] Yongzhen Huang,[1] Xianyong Lan,[1] Chuzhao Lei,[1] Yun Ma,[2] Linyong Hu,[3] and Hong Chen[1]

[1]Shaanxi Key Laboratory of Molecular Biology for Agriculture, College of Animal Science and Technology, Northwest A&F University, Shaanxi 712100, China; [2]College of Life Sciences, Xinyang Normal University, Institute for Conservation and Utilization of Agro-Bioresources in Dabie Mountains, Xinyang, Henan 464000, China; [3]Key Laboratory of Adaptation and Evolution of Plateau Biota, Northwest Institute of Plateau Biology, Chinese Academy of Sciences, Xining, Qinghai 810001, China

Muscle development is regulated by a series of complicate processes, and non-coding RNAs (ncRNAs) such as lncRNA have been reported to play important roles in regulating skeletal myogenesis and diseases. Here we profile the expression of lncRNA in cattle skeletal muscle tissue from fetus and adult developmental stages and detect 13,580 lncRNA candidates. Many of these lncRNAs are differentially expressed between two developmental stages. We further characterize one abundant lncRNA with the highest expression level of all downregulated lncRNAs, which we named muscle differentiation-associated lncRNA (MDNCR). Via luciferase screening, RNA binding protein immunoprecipitation (RIP), and RNA pull-down assays, MDNCR was observed to directly bind to miR-133a with 32 potential binding sites. GosB was identified as a target of miR-133a by luciferase activity, quantitative real-time qPCR, and western blotting assays. Overexpression of MDNCR increased the expression of GosB, whereas this effect was abolished by miR-133a. We found that MDNCR promotes myoblast differentiation and inhibits cell proliferation by sponging miR-133a. These results demonstrate that MDNCR binding miR-133a promotes cell differentiation by targeting GosB in cattle primary myoblasts.

INTRODUCTION

Over the past decade, genome-wide analyses of mammalian transcriptomes discovered that more than 50% of transcripts are not translated into proteins but act as transcriptional noise or functional RNAs, including non-coding RNA (ncRNA).[1,2] Generally, ncRNAs are divided into small or short ncRNA and long ncRNAs (lncRNAs). lncRNAs are usually identified as having an arbitrary minimum length of 200 nt and mostly have weak protein coding potential with lower expression levels than mRNA.[3,4] In recent years, a large number of lncRNAs has been identified in eukaryotic organisms from nematodes to humans,[5–9] and research is now concentrating on exploring their functions, revealing that lncRNAs play diverse roles in regulating biological processes such as cell differentiation,[10–12] transcriptional regulation,[13–15] and development[16–18] as well as in some diseases.[19–21]

Skeletal muscle tissue accounts for about 40% of adult human body weight and contributes to regulating metabolism and homeostasis. The formation and maintenance of muscle tissue are due to skeletal muscle myogenesis and regeneration. Numerous studies have demonstrated that lncRNAs regulates skeletal myogenesis and regeneration through versatile gene-regulatory mechanisms.[22–25] The majority of lncRNAs are engaged in epigenetic or transcriptional regulation on chromatins via their ability to interact with chromatin regulators.[22] For example, some lncRNAs assemble and recruit protein complexes, acting as a "molecular scaffold" to target genes, thereby activating or repressing transcription of target genes,[23,26] whereas other lncRNAs act as decoys to sequester transcriptional regulators and suppress their activity.[24,27] In addition, lncRNAs can also modulate post-transcriptional regulation in myogenesis, for example, by acting as sponges of microRNAs (miRNAs) to titrate them away from their target mRNAs; thus, they are called competing endogenous RNAs (ceRNAs).[10,28] Others generated from the antisense strand of coding genes can directly regulate the mRNA translation of the coding gene.[29,30] Moreover, several studies have demonstrated that some lncRNAs can encode micropeptides (<100 amino acids) to play micropeptide-mediated roles.[31,32] These findings demonstrate the critical role of lncRNAs in myogenesis through diverse regulatory mechanisms. Nevertheless, research regarding lncRNA involvement in myogenesis is still in its infancy, especially in livestock muscle differentiation; for example, in cattle.

Qinchuan cattle, known as the best Chinese yellow cattle, has excellent meat qualities.[33,34] The aim of this study was to identify lncRNAs with potential roles in Qinchuan cattle muscle growth

Received 20 April 2018; accepted 3 July 2018;
https://doi.org/10.1016/j.omtn.2018.07.003.

[4]These authors contributed equally to this work.

Correspondence: Hong Chen, Shaanxi Key Laboratory of Molecular Biology for Agriculture, College of Animal Science and Technology, Northwest A&F University, Shaanxi 712100, China.
E-mail: chenhong1212@263.net

Table 1. Summary of Reads Mapping to the Reference Genome

Samples	Fetus 1	Fetus 2	Fetus 3	Adult 1	Adult 2	Adult 3
Raw reads	111,340,382	106,866,166	134,501,982	139,160,360	101,780,186	101,084,070
Clean reads	88,317,616	80,238,976	104,670,312	108,467,672	85,317,802	84,111,208
Mapped reads	54,979,060	49,922,182	62,333,225	88,546,667	53,810,383	58,188,271
Mapping ratio	68.31%	68.17%	70.01%	84.18%	83.67%	84.47%
Uniquely mapped reads	50,334,911	45,233,401	57,170,376	86,082,724	52,330,653	56,687,937
Uniquely mapping ratio	62.54%	61.77%	64.21%	81.84%	81.37%	82.29%

and development. In this study, the Ribo-Zero RNA sequencing (RNA-seq) method[35,36] was used to analyze the fetus and adult *musculus longissimus* of Qinchuan cattle in the whole transcriptome with an unparalleled depth. 13,580 lncRNA candidates were obtained from cattle fetus and adult skeletal muscle samples, of which a number of lncRNAs were highly abundant, and 2,944 lncRNAs were differentially expressed between two developmental stages. We further characterize one abundant and muscle-specific lncRNA, termed muscle differentiation-associated lncRNA (MDNCR), which functions as a ceRNA for miR-133a and promotes myoblast differentiation and, thereby, augments the expression of its target gene GosB. Our study will extensively benefit the improvement of beef cattle breeding in China and provide new insight, describing the genetic mechanism of the excellent meat quality of Qinchuan cattle.

RESULTS

Profile of lncRNA Expression in Cattle Muscle

To identify the putative transcripts in cattle skeletal muscle, six *longissimus* muscle samples were obtained from Qinchuan cattle at the fetus stage (90 days) and adult stage (24 months old). In total, we acquired 45∼57 and 52∼86 million unique mapped clean reads from the fetus stage and adult stage libraries, respectively (Table 1). A large number of lncRNAs was identified in cattle muscle according to the steps of the workflow shown in Figure 1A. A total of 13,580 candidates were identified, and 9,161 were commonly expressed, whereas 4,343 and 76 were stage-specific at the fetus and adult stages, respectively (Figure 1B; Table S1). According to the cuffcompare classes, we found that most of the candidates (12,957) aligned to intergenic regions (u) (Table S1). We found that the distribution of detected lncRNAs is not uniform in chromosomes, but as a whole, the number of reads located in the chromosome increased with the increase in chromosome length (Figure 1C). Previous reports have shown that lncRNAs were shorter than protein-coding transcripts.[36] As illustrated in Figure 1D and Table 2, the mean length of lncRNAs was 1,645 nt, which was shorter than the mRNA (2,405 nt). However, it is worth mentioning that only 410 lncRNAs have an expression level of FPKM (the number of uniquely mapped fragments per kilobase of exon per million fragments mapped) > 1. The expression level of most lncRNAs (n = 13,490) was not higher than 50 spliced reads (FPKM; Figure 1E) and approximately 15-fold lower than that of the mRNA (1.7 versus 25.7).

Identification of Differentially Expressed lncRNA

We found that 2,944 lncRNAs were significantly different ($p < 0.05$) between the fetus stage and adult stage libraries, and all differentially expressed lncRNAs are provided in Table S2. The top 10 most highly expressed lncRNAs in the adult stage or fetus stage are shown in Tables 3 and 4, respectively. Of all differentially expressed lncRNAs, TCONS_00046501 showed the highest expression level of all upregulated lncRNAs, and TCONS_00238678 had the highest expression level of all downregulated lncRNAs in the adult sample compared with the fetus sample.

To further identify the potential roles of lncRNA, see the clustered heatmap in Figure S1. 826 lncRNAs were upregulated at least 2-fold, whereas 2,095 lncRNAs were downregulated when comparing adult with fetus muscle tissue ($p < 0.05$; Table S2). Scatterplot and volcano plot assays of lncRNA expression during muscle development showed that, from fetus stage to adult stage, many lncRNAs showed expression variation, and the fetus stage showed a clear preference for high lncRNA expression (Figures 2A and 2B).

GO and KEGG Pathway Analysis

lncRNAs can regulate the expression of nearby protein-coding genes and, thus, may execute functions to embody in the related mRNAs. Differentially regulated mRNA gene ontology (GO) enrichment analysis can uncover the role of differentially expressed lncRNAs. In this study, 362 functional groups were categorized in GO enrichment of the nearby mRNA of significantly differentially expressed lncRNAs ($p < 0.05$; Table S3), and the top 20 GO functional annotations are shown in Figure 2C. In addition, our data showed that 190 pathways were enriched, and the proteasome (ko03050) had the highest level of significance with 14 annotated genes, followed by basal transcription factors (ko03022) and nucleotide excision repair (ko03420) ($p < 0.05$; Table S4). The top 20 enriched Kyoto Encyclopedia of Genes and Genomes (KEGG) pathways are presented in Figure 2D. The results indicate that these pathways may contribute significantly to skeletal myogenesis.

Co-expression of lncRNAs and mRNAs

lncRNAs are a novel family of non-coding RNAs, and the potential for functionality of most lncRNAs is currently uncharacterized. To further investigate whether lncRNAs regulate transcription of

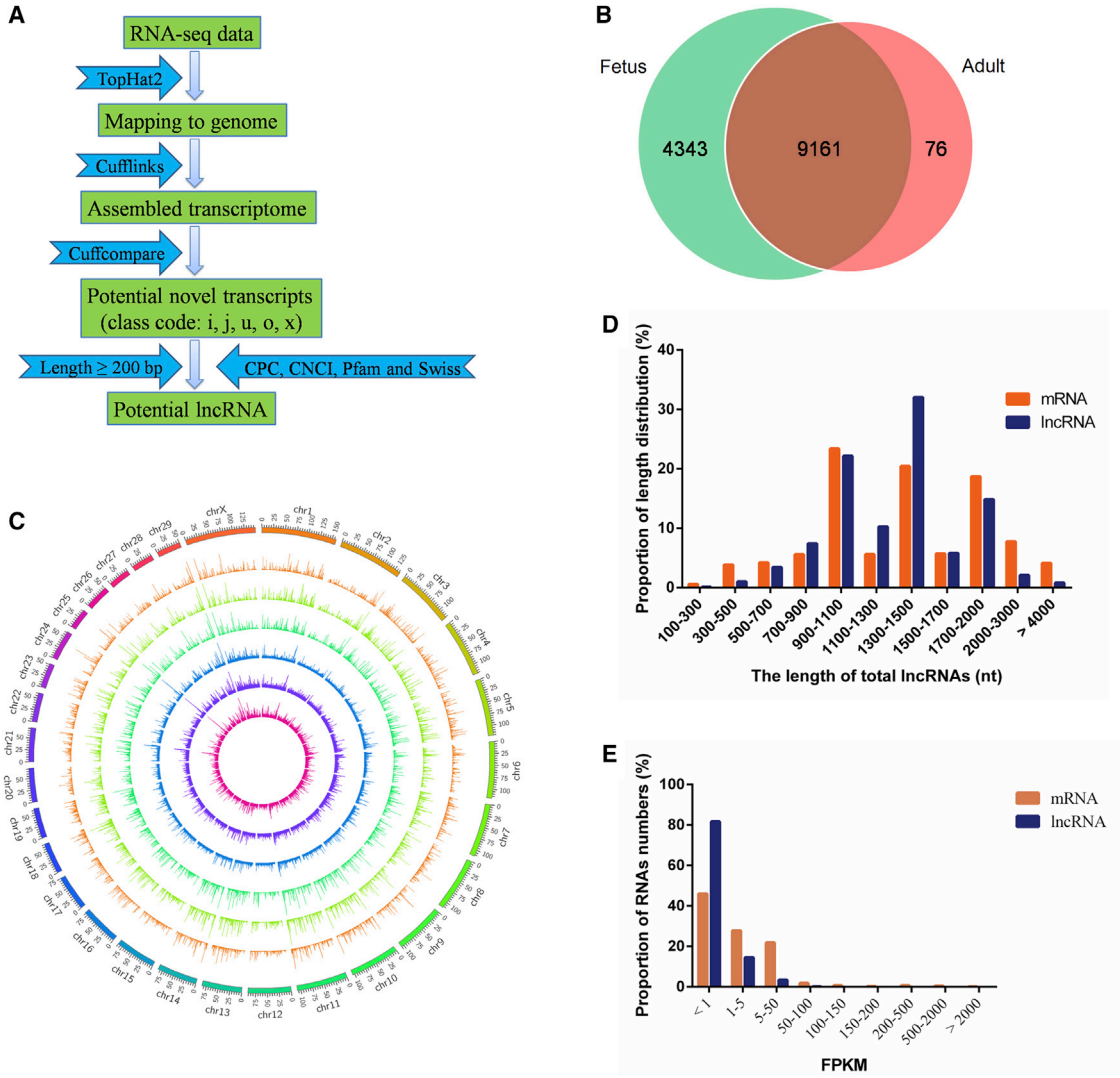

Figure 1. Identification of lncRNAs in Cattle Skeletal Muscle Tissue

(A) Workflow for the preparation and analysis of lncRNA libraries. (B) Venn diagram depicting different lncRNAs uncovered at two developmental stages (fetus and adult tissues). (C) Circos plot showing the distribution of lncRNAs in different chromosomes. (D) Size distribution of lncRNAs and protein-coding genes. (E) Comparison of the expression levels of mRNA and lncRNAs.

their potential targets (*cis*-regulatory relationships), we performed a co-expression analysis of the genes 100 kb upstream and downstream of the candidate lncRNAs. In this study, the potential function of lncRNAs was predicted using the annotated co-expressed mRNA function. Ten lncRNAs were chosen to search their neighboring coding genes (Figure 3A). For example, upregulation of TCONS_00076927 had a maximum number of 12 nearby coding genes, whereas downregulation of TCONS_00238678 had only one adjacent coding gene (MRPL23) and was negatively correlated with expression levels of MRPL23. The co-expression network could provide valuable information regarding these lncRNAs' potential functionality in regulating neighboring coding genes.

Table 2. Assembly Results of lncRNAs

Item	Min Length	Mean Length	Median Length	N50	Max Length
lncRNA	200	1,645	1,281	1,701	114,502
mRNA	201	2,405	1,808	3,166	103,350

ceRNA Network

lncRNAs, as miRNA sponges, may be members of ceRNAs, and we selected muscle development-related miRNAs and predicted their binding mRNAs. According to the common target miRNAs of lncRNAs and mRNAs, we constructed a ceRNA (mRNA-miRNA-lncRNA) network in cattle muscle with a total of 5 lncRNAs,

Table 3. The Top 10 Most Highly Expressed lncRNAs at the Adult Stage

lncRNA ID	Adult (FPKM)	Fetus (FPKM)	log2 (Adult/Fetus)	p Value
TCONS_00046501	930.28	161.626	2.52501	2.60E−01
TCONS_00238678	734.74	2,070.16	−1.49443	5.00E−05
TCONS_00353988	643.24	45.7731	3.81279	5.00E−05
TCONS_00076927	491.09	8.89745	5.78644	5.00E−05
TCONS_00203245	475.98	0.48976	9.92462	1.03E−01
TCONS_00046500	324.10	112.041	1.53239	9.26E−02
TCONS_00122369	286.90	12.4482	4.52652	1.95E−02
TCONS_00158520	276.36	20.9512	3.72146	5.00E−05
TCONS_00334157	265.42	2.81602	6.55847	5.00E−05
TCONS_00357835	260.72	14.1839	4.20016	1.22E−02

Table 4. The Top 10 Most Highly Expressed lncRNAs at the Fetus Stage

lncRNA ID	Adult (FPKM)	Fetus (FPKM)	log2 (Adult/Fetus)	p Value
TCONS_00238678	734.74	2,070.16	−1.49443	5.00E−05
TCONS_00212257	230.29	1,028.74	−2.15935	5.00E−05
TCONS_00212258	230.29	1,028.74	−2.15935	5.00E−05
TCONS_00212256	230.29	1,028.74	−2.15935	1.00E−04
TCONS_00208209	136.48	588.016	−2.10715	5.00E−05
TCONS_00007938	26.15	291.918	−3.48091	2.80E−02
TCONS_00173508	3.43	267.587	−6.28768	3.13E−01
TCONS_00208217	15.11	234.682	−3.95751	5.00E−05
TCONS_00173510	2.01	176.685	−6.45931	3.97E−01
TCONS_00240756	9.21	173.395	−4.23412	5.00E−05

44 mRNAs, and 16 miRNAs (Figure 3B). This ceRNA network may provide a novel perspective for cattle skeletal myogenesis.

Identification of the lncRNA MDNCR as a Candidate lncRNA

To identify specific lncRNAs displaying development-related changes in abundance, 15 differentially expressed lncRNAs were randomly selected and detected by real-time qPCR with 3 biological replicates. The normalized read counts of the selected 15 lncRNAs from the lncRNA-seq analysis are shown in Figure 4A. Validation of the lncRNAs by qPCR analysis exhibited upregulation and downregulation of these 15 lncRNAs (Figure 4B), and the chosen lncRNAs showed similar expression patterns between sequencing results and qPCR, suggesting that the lncRNA-seq data are highly accurate. The tissue expression assay showed that the expression of TCONS_00238678 was high in *longissimus* muscle, and its expression was much higher (146.7-fold) at the fetus stage compared with the adult stage, revealing potential roles in cattle muscle development (Figure 4B). We found that TCONS_00238678 was highly expressed in muscle tissue (Figure 4C). 5′ and 3′ rapid amplification of cDNA ends (RACE) analyses revealed that the full length of TCONS_00238678 was 1,974 nucleotides (Figure 4D; Text S1). Finally, we focused on TCONS_00238678, which we renamed MDNCR, to further explore its role in skeletal myogenesis.

MDNCR Acts as a ceRNA for miR-133a

Given that lncRNAs regulate gene expression post-transcriptionally by acting as miRNA sponges,[10,28] we next explored the ability of MDNCR-binding miRNAs. We transfected pcDNA-MDNCR into cattle primary myoblasts and found that MDNCR overexpression led to a more than 40-fold induction of MDNCR RNA (Figure 5A). The RNAhybrid and TargetScan software packages were used for miRNA binding analysis and suggested that MDNCR had 32 putative miR-133a binding sites (Figure 5B; Text S2). To determine the binding between MDNCR and miR-133a, we generated a miR-133a sensor by inserting two copies of the miRNA-133a complementary sequence downstream of the Rluc gene of the psiCHECK-2 vector (Figures 5C–5E). We found that miR-133a markedly decreased the Rluc activity of the miR-133a sensor and pCK-MDNCR-W in HEK293T cells. MDNCR recovered the reduced Rluc activity induced by miR-133a in a dose-dependent manner (Figure 5D), revealing that MDNCR could sponge miR-133a, thereby reversing the Rluc activity.

To confirm that MDNCR could bind directly to miR-133a, an RNA binding protein immunoprecipitation (RIP) assay was performed using Ago2 antibody, followed by semiquantitative PCR, confirming the interaction between MDNCR and miR-133a (Figure 5F). Furthermore, biotinylated miR-133a pull-down was performed to provide further evidence for MDNCR as a candidate ceRNA, and we found a more than 3-fold enrichment of MDNCR in the miR-133a-captured sample compared with the negative control (Figure 5G).

We speculated and screened GosB as a potential target gene of miR-133a with the bioinformatics software programs RNAhybrid and TargetScan. GosB has a highly conserved binding site in the mRNA 3′ UTR that has 18 putative miR-133a binding sites (Figure 6A; Text S3). Using a dual luciferase activity assay, we found that miR-133a could significantly decrease *Renilla* luciferase activity in co-transfect with miR-133a mimic and pCK-GosB-3′ UTR-W (Figure 6B). Moreover, MDNCR recovered the reduced Rluc activity induced by miR-133a. Similarly, we found that miR-133a markedly suppressed the expression of GosB at the protein level (Figures 6C and 6D). To confirm MDNCR acting as a ceRNA to relieve the miRNA-inhibiting effect on GosB, the cattle myoblasts were treated with pcDNA-MDNCR and/or the miR-133a mimic. Via western blotting and immunofluorescence assays, we found that MDNCR markedly promoted GosB expression, and this effect was abrogated by miR-133a overexpression (Figures 6D–6F).

miR-133a, which promotes myoblast proliferation and inhibits differentiation, is one of the best-characterized muscle-relevant miRNAs.[37,38] We showed that GosB was one target gene of

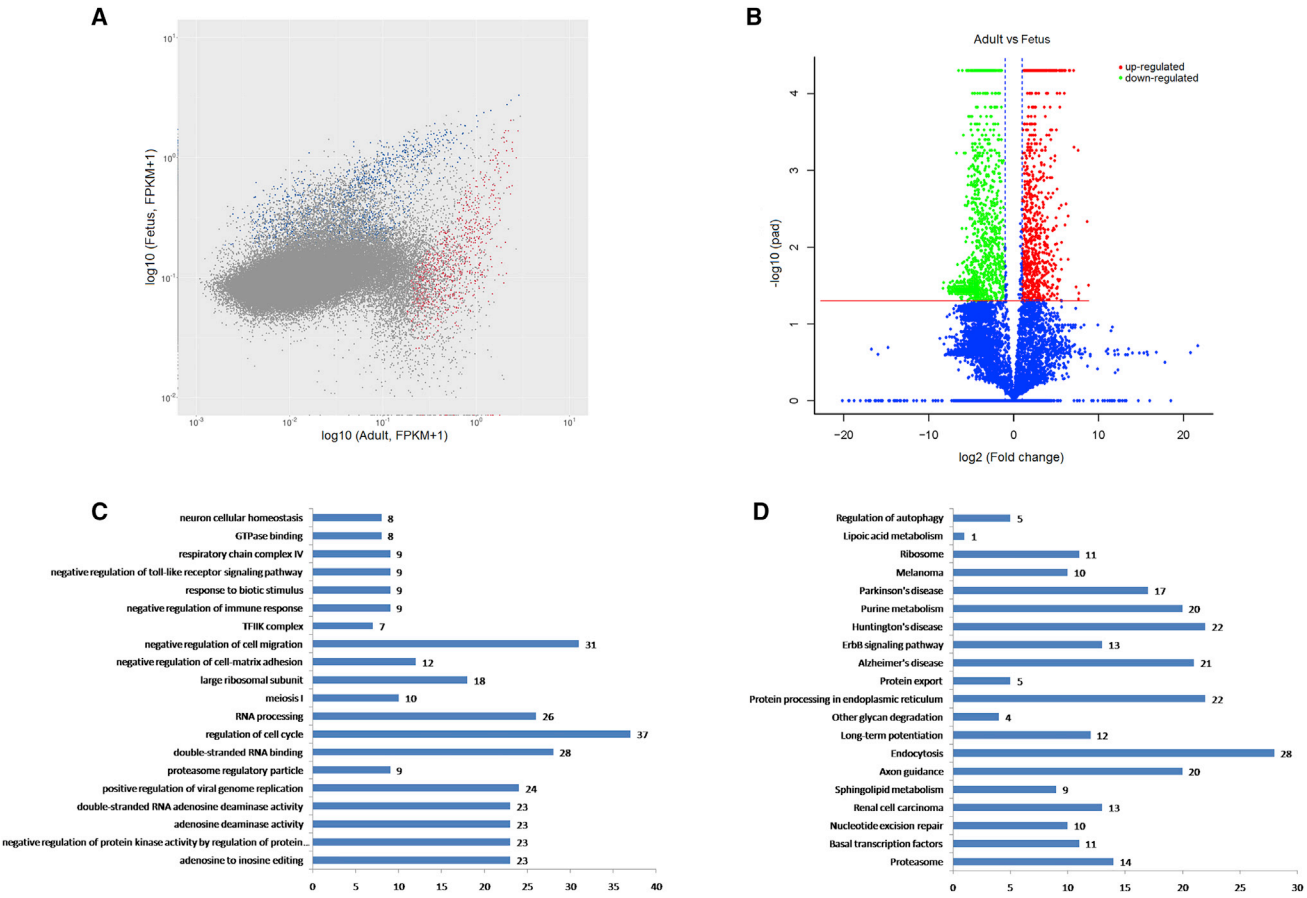

Figure 2. Differentially Expressed lncRNAs in Cattle Skeletal Muscle

(A and B) Scatterplot (A) and volcano plot (B) showing the correlation between abundance of individual lncRNAs at the fetus and adult stage. (C and D) Shown are the top 20 (C) gene ontology (GO) and (D) Kyoto Encyclopedia of Genes and Genomes (KEGG) terms of nearby mRNAs of significantly differentially expressed lncRNAs that were uncovered.

miR-133a, and then we asked whether GosB could affect myogenic differentiation. As shown in Figure 7, overexpression of GosB significantly promoted MyhC expression and induced myotube formation ($p < 0.05$), and siGosB inhibited the differentiation of cattle primary myocytes. Together, these findings reveal that MDNCR acts as a decoy to relieve the miR-133a-mediated inhibiting effect on GosB.

Effects of MDNCR on Myoblast Differentiation

To assess the effect of MDNCR on myoblast differentiation, the expression of established myogenic markers, MyoD, myogenin (MyoG), and myosin heavy chain (MyHC), was detected in primary cattle myoblasts treated with pcDNA-MDNCR or the miR-133a mimic and differentiated for 4 days. We found that the mRNA expression of MyoD, MyoG, and MyhC increased on day 4 relative to day 0, and the expression of MDNCR also significantly increased in cattle primary myoblasts differentiated for 4 days (Figures 8A and 8B). As seen in the immunofluorescence assay shown in Figures 8C and 8D, MDNCR markedly promoted MyhC expression and induced myotube formation. Using qPCR and western blotting assays, we found that miR-133a decreased the expression of MyoD and MyoG at the mRNA and protein levels, and these effects were abolished by overexpression of MDNCR (Figures 8E and 8F). These results demonstrate that MDNCR promotes myogenesis by binding miR-133a.

Effects of MDNCR on Myoblast Proliferation

To reveal the role of MDNCR in cattle myoblast proliferation, cell counting kit-8 (CCK-8), 5-Ethynyl-2'- deoxyuridine (EdU), qPCR, and western blotting assays were used. A cell phase assay revealed that MDNCR increased the proportion of cells in G0/G1 phase and decreased the number of myoblasts in S and G2 phases, suggesting that MDNCR may inhibit cell proliferation (Figures 9A and 9B). The CCK-8 assay revealed that MDNCR could significantly inhibit cell viability ($p < 0.05$; Figure 9C). The EdU assay had similar results (Figures 9D and 9E). We also detected the effect of MDNCR on expression of the cell proliferation-related genes CyclinD1 and proliferating cell nuclear antigen (PCNA) and found that MDNCR

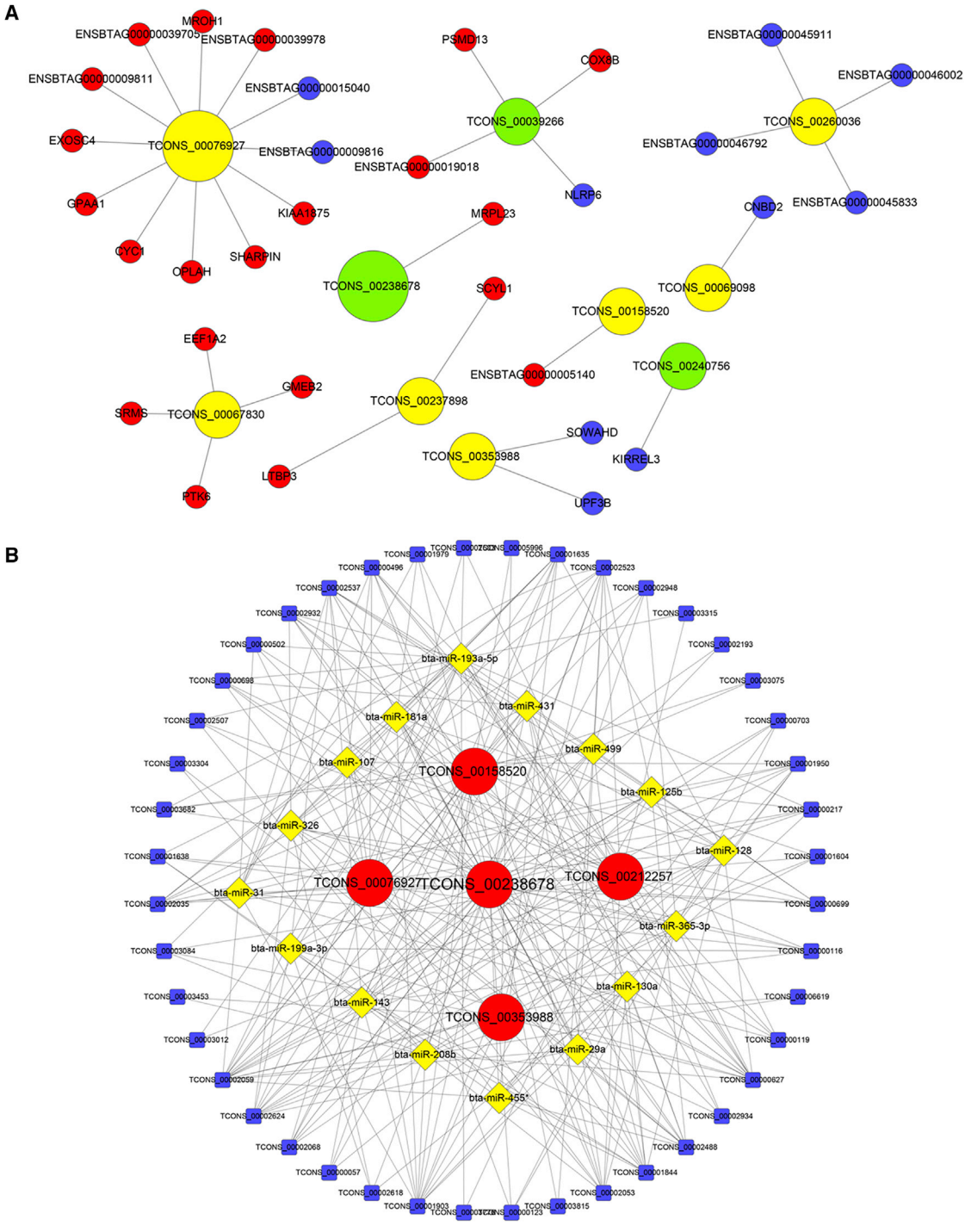

Figure 3. Co-expression Network and Competing Endogenous RNA Network in Cattle Muscle Tissues

(A) lncRNAs and their potential *cis*-regulated nearby genes are shown in the network. The large yellow nodes represent the upregulated lncRNAs, and the large green nodes represent the downregulated lncRNAs. The tiny red nodes indicate upregulated genes, and the tiny blue nodes indicate downregulated genes. (B) The network includes lncRNA-miRNA and miRNA-mRNA interactions; edges indicate sequence matching, and lncRNAs connect ties, suggesting miRNA-mediated mRNA expression.

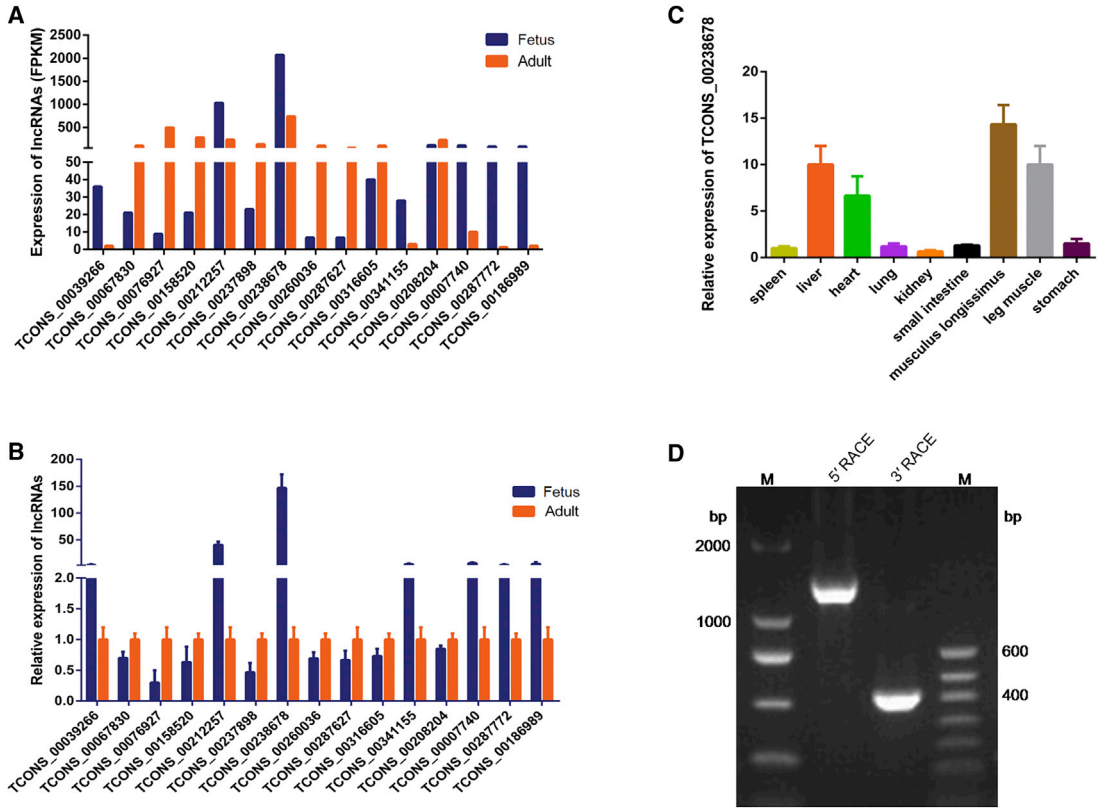

Figure 4. Validation of Putative lncRNAs

(A) 15 lncRNAs that were selected because they exhibited significantly different expression patterns (as assessed with our RNA-seq approach) when comparing two development stages. (B) Validation of differential expression of lncRNAs using real-time qPCR; 15 lncRNAs confirmed the predicted pattern. (C) Expression levels of the candidate lncRNA TCONS_00238678 in different tissues of cattle fetus. (D) 5′ and 3′ RACE of TCONS_00238678 (renamed MDNCR) in muscle samples. Values are means ± SEM for three individuals.

significantly decreased the expression of these genes at the mRNA and protein levels (Figures 9F and 9G). We also found that miR-133a promoted cell proliferation, and pretreatment of cattle primary myoblasts with the miR-133a mimic followed by MDNCR overexpression resulted in negligible effects on cell proliferation, revealing that MDNCR abrogates the effect of miR-133a on cell proliferation. These results confirm that MDNCR inhibits cell proliferation by sponging miR-133a.

Effects of MDNCR on Cell Apoptosis

Research has shown that miR-133a inhibits myoblast apoptosis;[39] thus, we wanted to know whether MDNCR could regulate myoblast apoptosis by sponging miR-133a. Hoechst 33342 and propidium iodide (PI) and Annexin V-fluorescein isothiocyanate (FITC) and PI dual staining assays showed that MDNCR relieved the protection effect of primary cattle myoblasts induced by miR-133a overexpression (Figures 10A–10C). Bcl-2 has been demonstrated to be a pro-survival protein, and we asked whether Bcl-2 participates in the survival-inhibiting effect of MDNCR in myoblasts; thus, the expression of Bcl-2 was quantified in cattle myoblasts pretreated with pcDNA-MDNCR and/or the miR-133a mimic. MDNCR inhibited the expression of *Bcl-2* while increasing the expression of *Bax* (Figure 10D). Consistently, MDNCR significantly increased the expression of caspase-3 and caspase-9 (Figure 10D). These results demonstrate that MDNCR binding miR-133a promotes myoblast differentiation and apoptosis by targeting GosB in cattle primary myoblasts (Figure 11).

DISCUSSION

Most studies exploring the molecular mechanisms of skeletal myogenesis in cattle focus on protein-coding genes; therefore, studies using high-throughput RNA-seq analysis usually investigate protein-coding genes. However, the occurrence and potential functions of lncRNAs in cattle myogenesis remain largely unknown. Using an RNA-seq method, a large number of lncRNAs were identified and annotated in Qinchuan cattle skeletal muscle. We found that most lncRNAs in cattle muscle tissue were of low expression and, accordingly, might be by-products of mRNA. Nevertheless, numerous abundant lncRNAs were differentially expressed between fetus and adult muscle tissues, which revealed

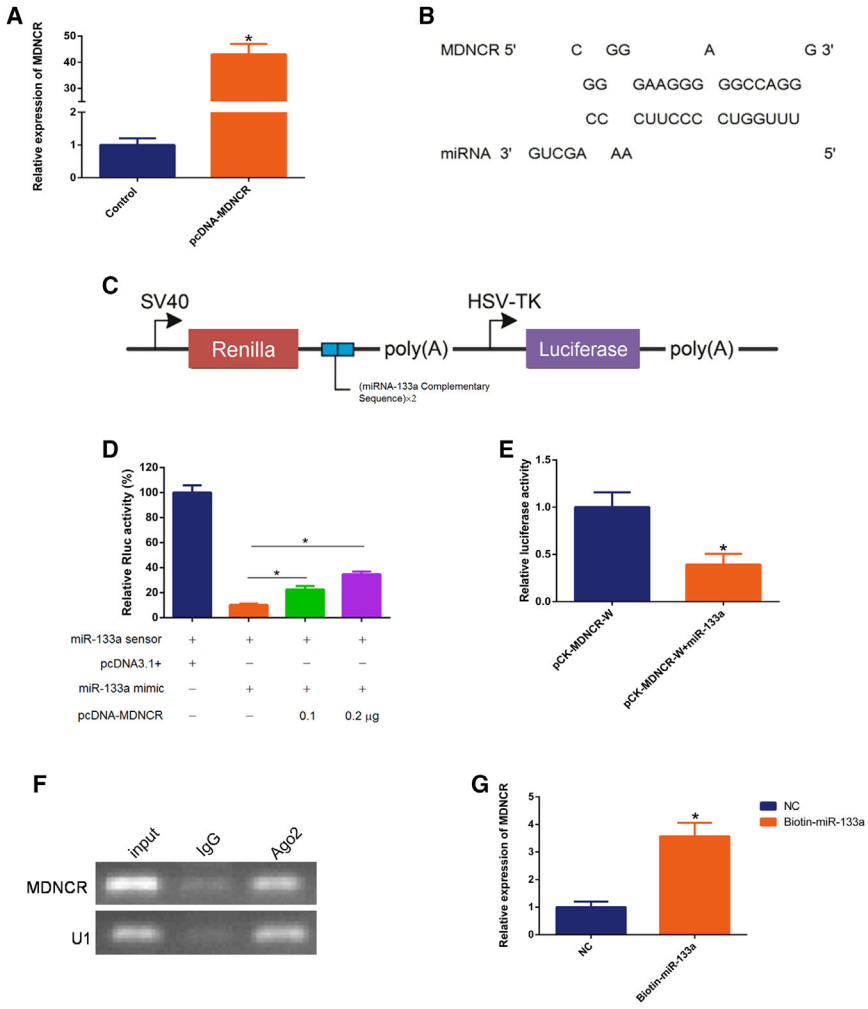

Figure 5. MDNCR Functions as a miRNA Sponge

(A) Visualization of the efficiency of the MDNCR overexpression vector pcDNA-MDNCR by real-time qPCR. (B) RNAhybrid and TargetScan predicted miR-133a binding sites at 32 distinct positions in MDNCR. (C) The miR-133a sensor construct. (D) The miR-133a sensor was co-transfected with the miR-133a mimic and/or pcDNA-MDNCR into cattle primary myocytes. *Renilla* luciferase activity was normalized to firefly luciferase activity. (E) The miR-133a mimic was co-transfected with pCK-MDNCR-W into cattle primary myocytes. (F) Association of MDNCR and miR-133a with Ago2. Cellular lysates were used for the RIP assay with Ago2 antibody. MDNCR and miR-133a levels were detected using semiquantitative PCR. (G) Biotin-labeled miRNA was purified and subjected to RNA pull-down assays by incubation with cattle primary myoblast lysates, followed by qPCR analysis of the MDNCR level. Values are means ± SEM for three individuals. *$p < 0.05$.

that they have a specific role in muscle. Furthermore, certain lncRNAs were predominately or specifically expressed in muscle (for example, MDNCR), which suggests that these lncRNAs are purposefully produced. Consistently, many studies have demonstrated that lncRNAs are not simply the by-products of protein coding genes, and many lncRNAs have been confirmed to play roles during skeletal myogenesis.[23,24,26,27]

Research increasingly suggests that lncRNAs are engaging in epigenetic or transcriptional regulation of neighboring genes in *cis* or in *trans*.[23,26] Hence, a network of 10 lncRNAs was chosen to search their adjacent coding genes, which may provide new evidence for understanding the lncRNAs' potential functionality in regulating neighboring coding genes. Downregulation of MDNCR had only 1 neighboring coding gene (MRPL23) and was negatively correlated with expression levels of MRPL23. According to the common target miRNAs of lncRNAs and mRNAs, an mRNA-miRNA-lncRNA network was constructed in cattle muscle. We showed that MDNCR had the highest expression level of all down-regulated lncRNAs. The tissue expression assay showed that the lncRNA MDNCR was expressed predominantly in muscle, revealing potential roles in cattle muscle development. Software prediction analysis showed that MDNCR contains 32 binding sites of miR-133a, which is one of the best-characterized muscle-relevant miRNAs. Thus, we focused on MDNCR to further explore its role in skeletal myogenesis and found that MDNCR could promote myoblast differentiation and apoptosis. Accumulating evidence indicates that lncRNAs can modulate post-transcriptional regulation; for example, by acting as sponges of miRNAs to titrate them away from their target mRNAs. Thus, they are called ceRNAs.[40–43] In this study, via software prediction, luciferase screening, and RNA pull-down and RIP assays, MDNCR was observed to sponge miR-133a.[37,38] We found that MDNCR and miR-133a in myoblasts produced an opposite effect in myoblast differentiation. Consistently, miR-133a protected myoblasts from apoptosis, and this effect could be abolished by MDNCR overexpression, suggesting that the MDNCR miRNA sponge effect works soundly. These results further demonstrate that MDNCR could serve as a regulator of skeletal myogenesis by sponging miR-133a.

Our study provides a catalog of lncRNA expression in cattle muscle tissues. Thousands of lncRNAs were annotated, several of which present a highly different abundance in fetus and adult muscle samples. We further characterized an abundant lncRNA—the most downregulated lncRNA, MDNCR. Our findings suggested MDNCR as a ceRNA to promote myogenesis by sponging miR-133a. We anticipate that these results will be a stepping stone to identifying the genetic

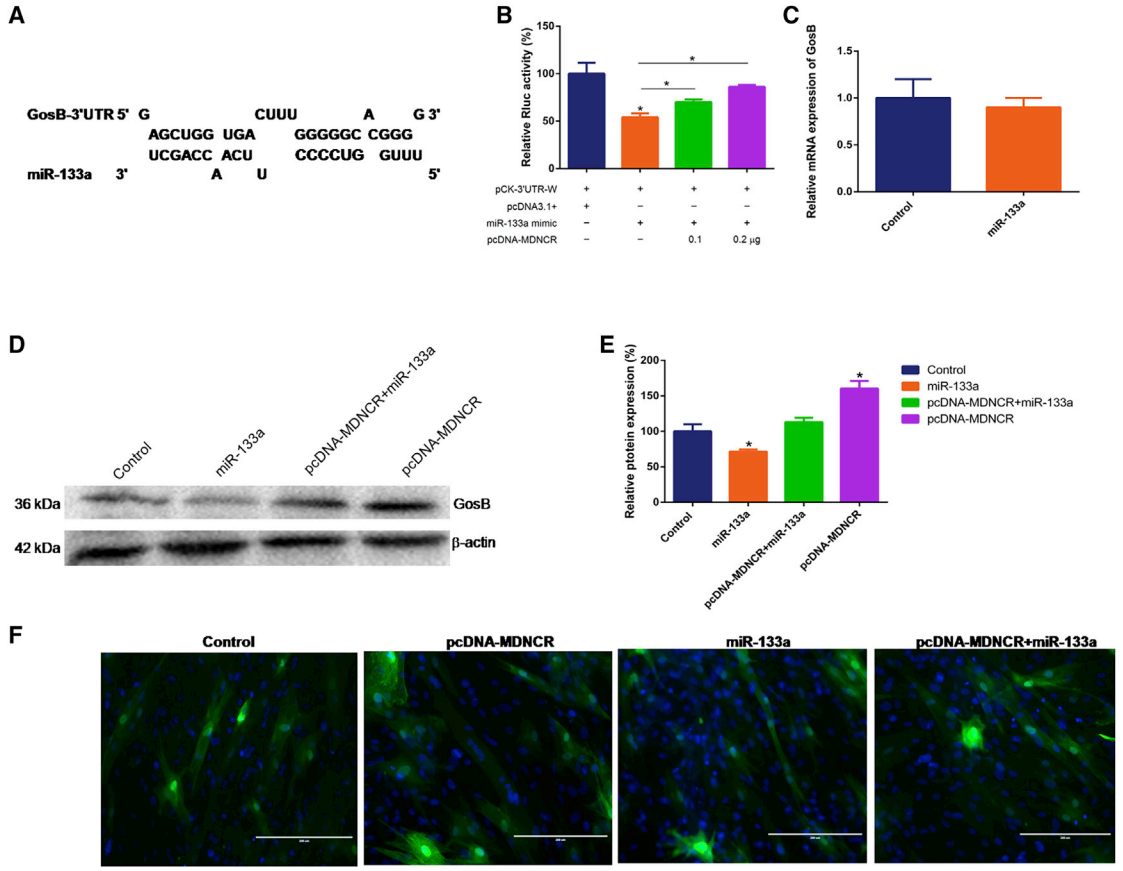

Figure 6. MDNCR Binding of miR-133a Relieves Its Inhibition of GosB

(A) RNAhybrid and TargetScan predicted miR-133a binding sites at 18 distinct positions in the GosB 3′ UTR. (B) Cells were co-transfected with the miR-133a mimic and pCK-GosB-3′ UTR-W or pcDNA-MDNCR, and *Renilla* luciferase activity was normalized to the firefly luciferase activity. (C) The mRNA expression of *GosB* was detected by real-time qPCR. (D and E) The protein expression of GosB was detected by western blotting (D), and protein band density was also analyzed (E). (F) The role of MDNCR as a ceRNA was detected by immunofluorescence (GosB) and observed under a fluorescence microscope. Scale bars represent 200 μm. Values are means ± SEM for three individuals. *$p < 0.05$.

mechanisms governing muscle formation and regeneration, which may be implemented in therapies for muscle diseases.

MATERIALS AND METHODS

Sample Preparation

Cattle fetuses (90 days) and adult Qinchuan cattle (24 months old) were obtained from a local slaughterhouse in Xi'An, China. In addition, we obtained heart, spleen, kidney, liver, lung, stomach, small intestine, and leg muscle tissues from fetuses. The tissues were taken with informed consent, and all procedures were approved by the No. 5 Proclamation of the Ministry of Agriculture, China.

Library Preparation and Sequencing Analysis

Total RNA was extracted from three fetal and three adult Qinchuan cattle *longissimus* muscles, assessed by electrophoresis, and quantified with an Agilent 2100 Bioanalyzer (Agilent Technologies, Santa Clara, CA, USA) and a NanoDrop spectrophotometer (NanoDrop, Wilmington, USA). Library preparation and Illumina sequencing analysis were described in a previous study.[44]

lncRNA Identification

Putative lncRNAs were identified with the following steps. Only transcripts of 200 bp or more and multi-exonic transcripts remained. Transcripts with 3 or fewer reads were removed. Among the cuffcompare classes, transcripts annotated as "i," "j," "o," "u," and "x," representing novel intronic, potentially novel isoform, generic exonic overlap with a reference transcript, intergenic, and antisense transcripts, respectively, were kept. The candidate lncRNAs with coding potential calculator (CPC) score < -1, and coding-non-coding-index (CNCI) score < 0 were remained. Transcripts with a predicted open reading frame (ORF) of more than 100 amino acids (aa) were removed. Transcripts containing a known protein-coding domain were removed by alignment with the Pfam and Swiss-Protein databases. The raw sequencing dataset supporting the results of this study

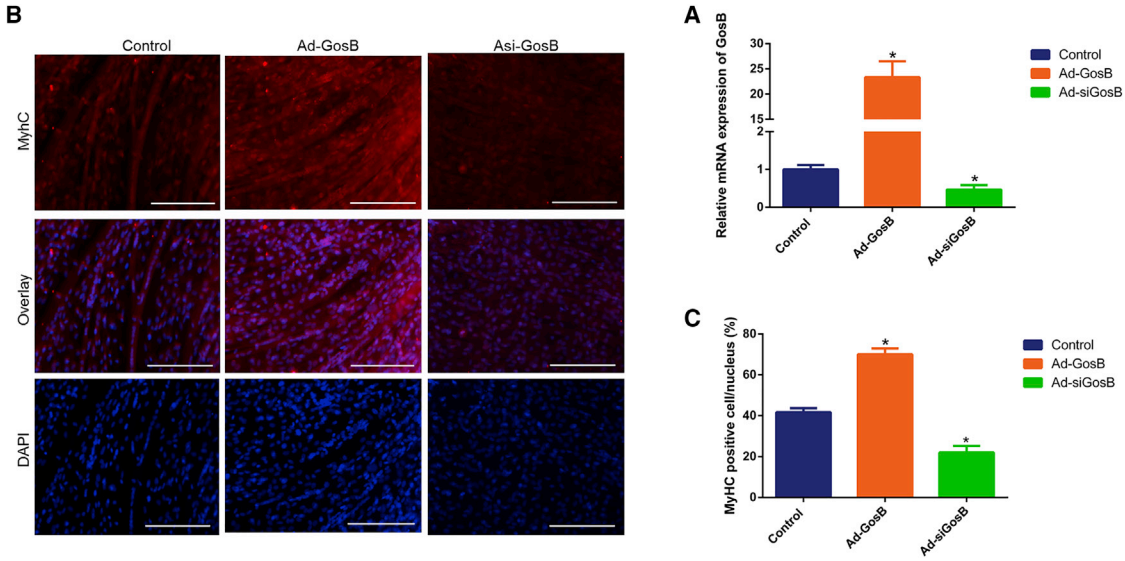

Figure 7. GosB Promotes the Differentiation of Cattle Primary Myocytes

(A) The expression of GosB was detected by qPCR. (B and C) Cell differentiation was detected by immunofluorescence (C, MyhC) and observed under a fluorescence microscope (B). Values are means ± SEM for three individuals. *p < 0.05.

was deposited in the NCBI GEO database (https://www.ncbi.nlm.nih.gov/geo/). The data are accessible through GEO: GSE86847 (https://www.ncbi.nlm.nih.gov/geo/query/acc.cgi?acc = GSE86847).

Gene Ontology and Pathway Analyses

Gene ontology analysis (http://www.geneontology.org) and KEGG (https://www.kegg.jp/) pathway analysis were performed as described in a previous study.[45]

Co-expression Analysis

lncRNA could be a *cis* regulator that regulates its nearby genes located at the same chromosome. We performed a co-expression analysis of the genes 100 kb upstream and downstream of the candidate lncRNAs. The enrichment or connectivity was due to position frequency matrix as described in a previous study.[46]

ceRNA Network Analysis

An mRNA-miRNA-lncRNA network was constructed based on the miRNA mature sequence binding sites on the mRNA and the lncRNAs. The interactions of miRNA-lncRNA and miRNA-mRNA were predicted by RNAhybrid (https://bibiserv.cebitec.uni-bielefeld.de/rnahybrid), TargetScan (http://www.targetscan.org/), and miRbase (http://www.mirbase.org/).

5′- and 3′ RACE

The full-length sequence of MDNCR was obtained using the SMARTer RACE cDNA Amplification Kit (Clontech Laboratories, Palo Alto, CA, USA) as described in a previous study.[36] The specific primers used for 5′ and 3′ RACE were 5′-GAAGTCCGTGTTCC AAGTCCCAGGC-3′ and 5′-CCCGGCCCGGCGACTCCATC-3′, respectively.

RNA Preparation and Real-Time qPCR

Total RNA extraction, cDNA synthesis, and qPCR were performed as described previously.[39,45] The qPCR analyses were performed using SYBR Green PCR Master Mix (Takara, Dalian, China). For each time point, qPCR was performed on three biological replicates. All qPCR tests were run on the RNA used for Illumina sequencing. *U6* (for miRNA) and *β-actin* were used as the internal controls for normalization of the data. The primers are listed in Table S5, and the $2^{-\Delta\Delta Ct}$ method was used to analyze the relative expression level of the qPCR data.

Vector Construction

The whole length of MDNCR was cloned into the overexpression vector of pcDNA-3.1(+) using PrimerSTAR Max DNA Polymerase Mix (Takara, Dalian, China). The fragment of the GosB 3′ UTR, including the binding site of miR-133a, was amplified and inserted into the psiCHECK-2 vector (Promega, Madison, WI, USA) at the 3′ end of the *Renilla* gene (pCK-GosB-3′ UTR-W). Similarly, the vectors of psi-CHECK-MDNCR-W (pCK-MDNCR-W) were obtained using the same method. A miR-133a sensor was generated by inserting two miR-133a complementary sequences into psiCHECK-2. The GosB overexpression recombinant adenovirus Ad-GosB and the interference expression recombinant adenovirus Ad-siGosB were prepared in our laboratory.[44] Primer sequences are shown in Table S5. All constructs were verified by sequencing.

Cell Treatment

Primary cattle myoblasts were isolated and cultured from cattle *longissimus* muscle as described previously.[44] For myoblast differentiation, myoblasts were grown to 80% confluence in growth medium (GM), followed by an exchange with differentiation medium (DM)

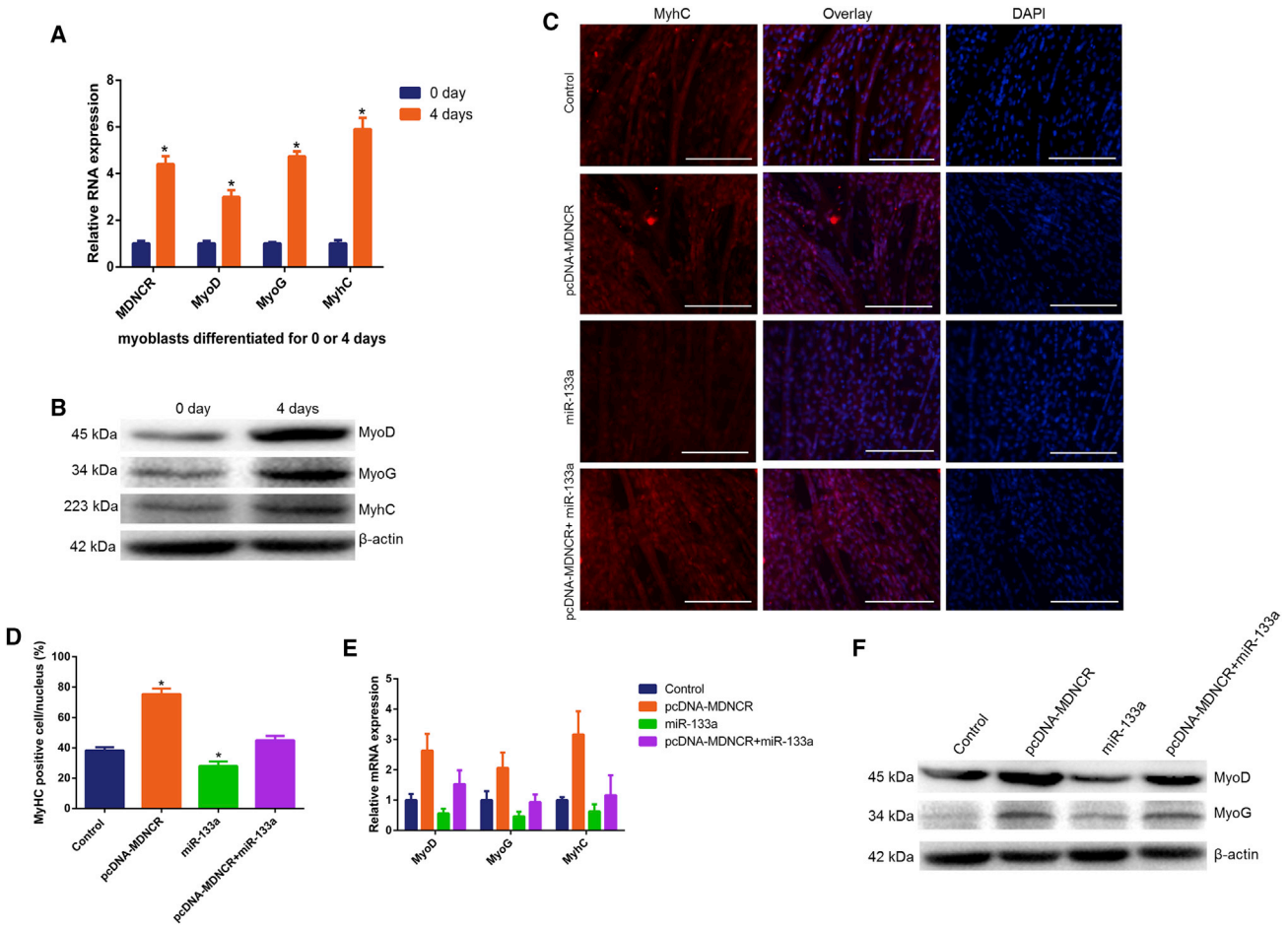

Figure 8. MDNCR Promotes the Differentiation of Cattle Primary Myocytes

(A and B) The expression levels of MDNCR, MyoD, MyoG, and MyhC in myoblasts differentiated for 0 and 4 days by (A) real-time qPCR and (B) western blotting, respectively. (C and D) Cattle primary myocytes were transfected with pcDNA-MDNCR and/or the miR-133a mimic, and cell differentiation was detected by immunofluorescence (D, MyhC) and observed under a fluorescence microscope (C). (E and F) Expression of the marker genes MyoD, MyoG, and MyhC for myocyte differentiation was detected by qPCR (E) and western blotting (F). Values are means ± SEM for three individuals. The scale bars represent 200 μm. *$p < 0.05$.

consisting of DMEM containing 2% heat-inactivated horse serum. The DM was exchanged every day. Myoblasts were transfected with the miR-133a mimic or pcDNA-MDNCR using TurboFect (R0531, Thermo Scientific, Waltham, USA) when cell confluence reached approximately 80%.

Cell Proliferation Assay

To gain insights into the effect of MDNCR on myoblast proliferation, EdU incorporation assays (Ribobio, Guangzhou, China) and CCK-8 (Multisciences, Hangzhou, China) were used, as described previously.[45]

Flow Cytometry for Cell Cycle and Apoptosis Assays

We analyzed the cell cycle using a cell cycle testing kit (Multisciences, Hangzhou, China), as described previously.[45] Cell apoptosis was measured by Annexin V-FITC and PI staining assay as described previously.[45]

Hoechst 33342 and PI Dual Staining Assays

Hoechst 33342 and PI double staining (Solarbio, Beijing, China) was performed to analyze cell apoptosis. In brief, after transfection with pcDNA-MDNCR or the miR-133a mimic for 24 hr, cells were incubated with Hoechst 33342 for 15 min at room temperature. Then the cells were treated with PI for 10 min at room temperature. The fluorescence signal was assessed using a fluorescence microscope (DM5000B, Leica Camera AG, Germany).

Luciferase Activity Assay

When the cell confluence reached about 80%, the miR-133a mimic, pcDNA-MDNCR, and pCK-GosB-3′ UTR-W were co-transfected into HEK293T cells. Similarly, the miR-133a mimic and pCK-MDNCR-W or miR-133a sensor were co-transfected into cells. After incubation for 24 hr, the cells were washed with PBS and harvested using 200 μL passive lysis buffer (PLB). Dual luciferase activity was

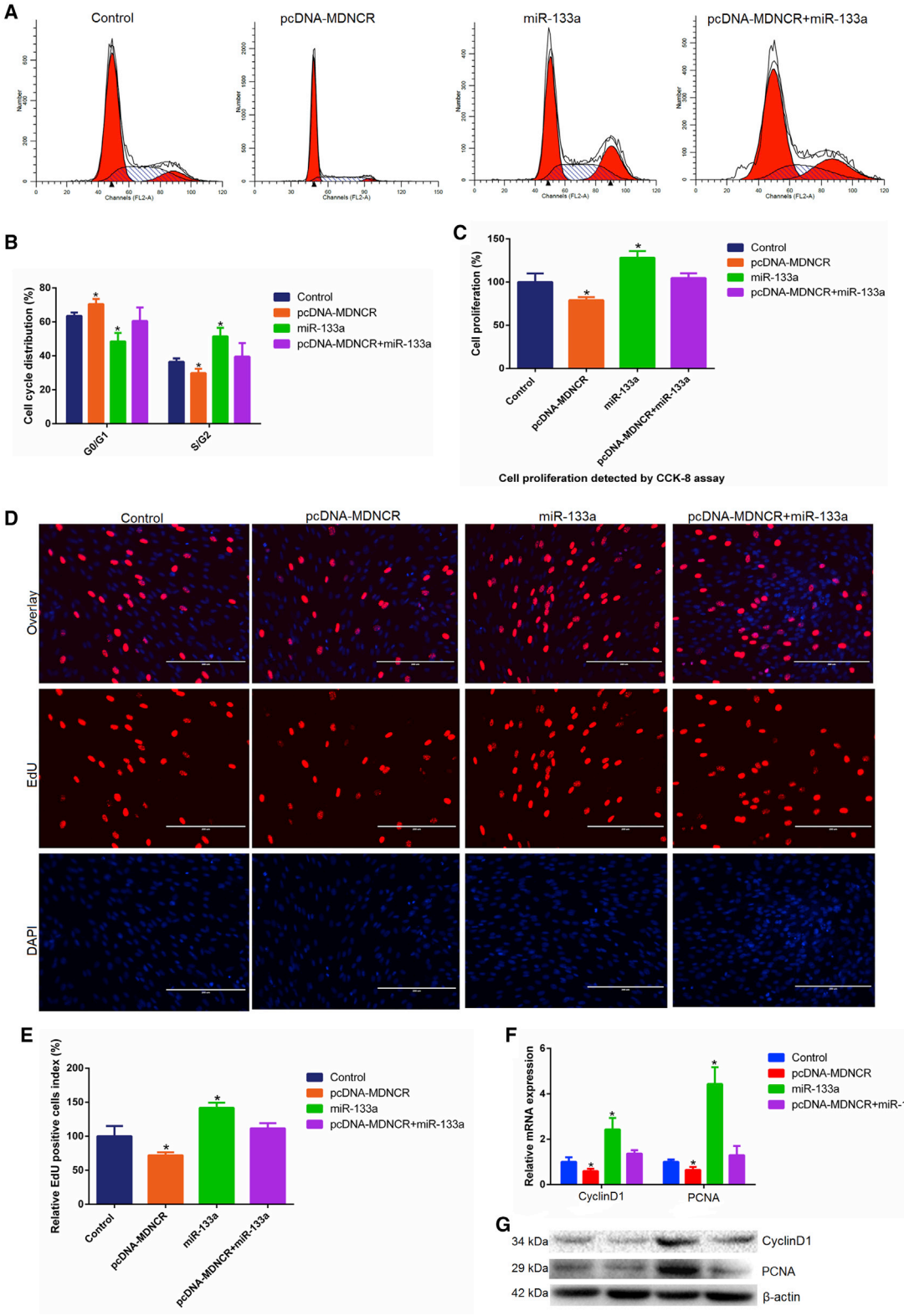

(legend on next page)

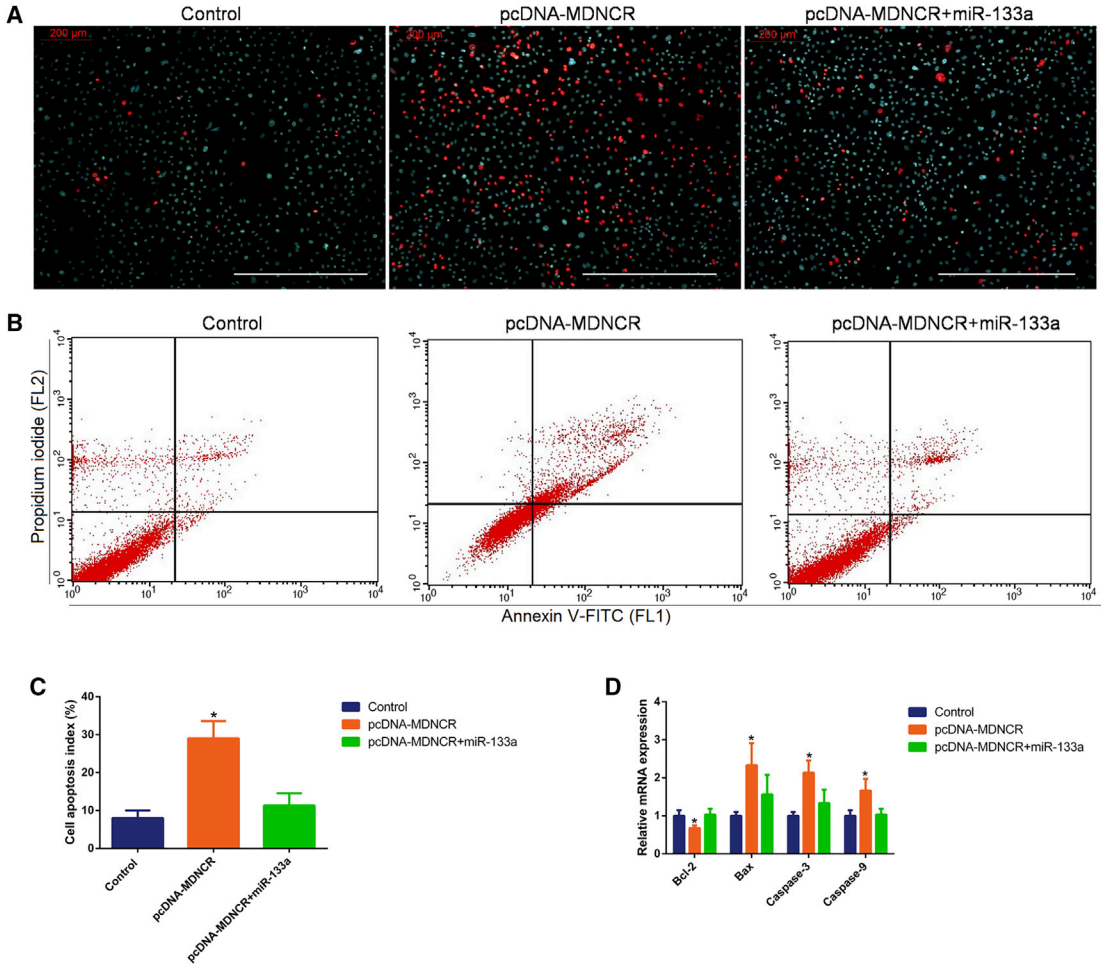

Figure 10. Effects of MDNCR on Cell Apoptosis

(A–C) Cell apoptosis was determined by Hoechst 33342 and PI dual staining assays (A) and Annexin V-FITC and PI binding followed by flow cytometry (B) and counted (C). (D) The mRNA of apoptosis marker genes (*Bcl-2*, *Bax*, *Caspase-9*, and *Caspase-3*) was detected using real-time qPCR. Scale bars represent 200 μm. Data are shown as means ± SEM for three individuals. *$p < 0.05$.

measured using an automatic microplate reader (Molecular Devices, Sunnyvale, USA), and *Renilla* luciferase activity was normalized against firefly luciferase activity.

Western Blotting

The total proteins were extracted from cells using the protein lysis buffer radioimmunoprecipitation assay (RIPA) containing 1 mM PMSF (Solarbio, Beijing, China). The extracts were boiled with 4× SDS loading buffer at 98°C for 10 min, and then 20 μg total protein was loaded and separated on 10% SDS-PAGE gels. After electrophoresis, the samples were transferred to a polyvinylidene fluoride (PVDF) membrane that was soaked in formaldehyde and then blocked with 5% skim milk for about 2 hr at room temperature. The membrane was then incubated overnight with primary antibodies specific for anti-MyoD, anti-MyHC, anti-MyoG, anti-PCNA, anti-CyclinD1 (Abcam, Cambridge, England), and anti-β-actin (Sungene Biotech, Tianjin, China) at 4°C. The PVDF membrane was washed three times with tris saline with tween (TBST) buffer and then incubated with secondary antibody for 2 hr at room temperature. β-Actin was used as the internal control with a

Figure 9. The Effect of MDNCR on Cell Proliferation

(A and B) Cattle primary myocytes were transfected with pcDNA-MDNCR and/or the miR-133a mimic. Cell phases were analyzed by flow cytometry (A) and counted (B). (C–E) Cell proliferation analysis using cell counting kit-8 (C, CKK-8) (C) and EdU incorporation assays (D) and EdU-positive cell index statistics are also shown (E). (F and G)The expression of proliferating cell nuclear antigen (PCNA) and CyclinD1 was detected by (F) real-time qPCR and (G) western blotting. Data are presented as means ± SEM for three individuals. Scale bars indicate 200 μm. *$p < 0.05$.

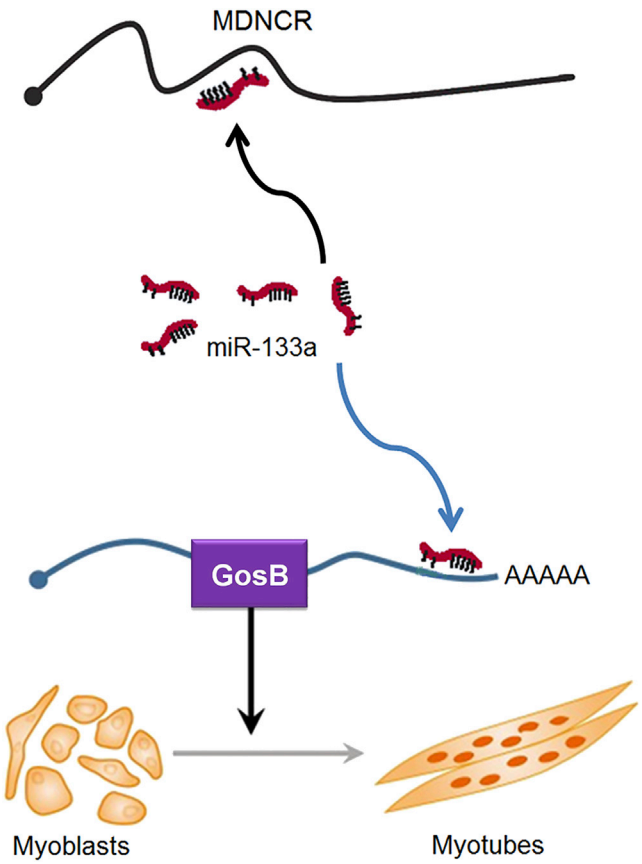

Figure 11. Proposed Model of MDNCR Regulation of Cattle Myoblast Differentiation

secondary antibody that was horseradish peroxidase (HRP)-labeled anti-mouse immunoglobulin G (IgG) (Sungene Biotech, China). Finally, antibody-reacting bands were detected using enhanced chemiluminescence (ECL) luminous fluid (Solarbio, China).

Immunofluorescence and Microscopy

Immunofluorescence assay was performed as described previously.[45] The fluorescence signal of the proteins GosB and MyHC was assessed using a fluorescence microscope (DM5000B, Leica Camera AG, Germany).

RIP Assay

The Magna RIP RNA-Binding Protein Immunoprecipitation Kit was used to perform the RIP assay (Millipore, Bedford, MA, USA) following the manufacturer's protocol. Briefly, primary cattle myoblasts were collected and lysed using RIP lysis buffer. Then cell lysates were incubated with magnetic beads conjugated with anti-Ago2 antibody (Abcam, Cambridge, England). Then the immunoprecipitated RNA was isolated, and the abundance of MDNCR and miR-133a in bound fractions was evaluated by qPCR analysis.

Biotin-Coupled miRNA Capture

The biotin-coupled miRNA pull-down assays were performed as described previously.[47,48] Briefly, the biotinylated miR-133a (Genseed, Guangzhou, China) was transfected into cattle primary myoblasts for 24 hr, and then the biotin-coupled RNA complex was pulled down by incubating the cell lysates with streptavidin-coated magnetic beads (Life Technologies, Carlsbad, CA). The abundance of MDNCR in bound fractions was evaluated by qPCR analysis.

Statistical Analysis

The quantitative results are presented as mean ± SEM based on at least three independent experiments. All data in this study were analyzed by one-way ANOVA for p value calculations using SPSS v17.0 software. $p < 0.05$ was considered statistically significant among means.

SUPPLEMENTAL INFORMATION

Supplemental Information includes one figure, five tables, and three text files and can be found with this article online at https://doi.org/10.1016/j.omtn.2018.07.003.

AUTHOR CONTRIBUTIONS

H.C., H.L., and X.W. designed the study. H.L., J.Y., and X.W. performed the experiments and drafted the manuscript. C.S., R.J., Z.H., and C.L. helped perform the experiments and analyzed the data. L.H., Y.M., and X.L. helped collect tissue samples.

CONFLICTS OF INTEREST

The authors declare no conflict of interest.

ACKNOWLEDGMENTS

This work was supported by National Natural Science Foundation of China grant 31772574, Program of National Beef Cattle and Yak Industrial Technology Systems grant CARS-37, Applied Basic Research Program of Qinghai Province grant 2014-ZJ-710, and Special Fund of Xinyang Normal University grant 2017001.

REFERENCES

1. Koufariotis, L.T., Chen, Y.-P.P., Chamberlain, A., Vander Jagt, C., and Hayes, B.J. (2015). A catalogue of novel bovine long noncoding RNA across 18 tissues. PLoS ONE *10*, e0141225.

2. Li, H., Wei, X., Yang, J., Dong, D., Hao, D., Huang, Y., Lan, X., Plath, M., Lei, C., Ma, Y., et al. (2018). circFGFR4 Promotes Differentiation of Myoblasts via Binding miR-107 to Relieve Its Inhibition of Wnt3a. Mol. Ther. Nucleic Acids *11*, 272–283.

3. Marques, A.C., and Ponting, C.P. (2014). Intergenic lncRNAs and the evolution of gene expression. Curr. Opin. Genet. Dev. *27*, 48–53.

4. Kaikkonen, M.U., Lam, M.T., and Glass, C.K. (2011). Non-coding RNAs as regulators of gene expression and epigenetics. Cardiovasc. Res. *90*, 430–440.

5. Nam, J.-W., and Bartel, D.P. (2012). Long noncoding RNAs in C. elegans. Genome Res. *22*, 2529–2540.

6. Pauli, A., Valen, E., Lin, M.F., Garber, M., Vastenhouw, N.L., Levin, J.Z., Fan, L., Sandelin, A., Rinn, J.L., Regev, A., and Schier, A.F. (2012). Systematic identification of long noncoding RNAs expressed during zebrafish embryogenesis. Genome Res. *22*, 577–591.

7. Li, T., Wang, S., Wu, R., Zhou, X., Zhu, D., and Zhang, Y. (2012). Identification of long non-protein coding RNAs in chicken skeletal muscle using next generation sequencing. Genomics *99*, 292–298.

8. Guttman, M., Garber, M., Levin, J.Z., Donaghey, J., Robinson, J., Adiconis, X., Fan, L., Koziol, M.J., Gnirke, A., Nusbaum, C., et al. (2010). Ab initio reconstruction of cell type-specific transcriptomes in mouse reveals the conserved multi-exonic structure of lincRNAs. Nat. Biotechnol. *28*, 503–510.

9. Bánfai, B., Jia, H., Khatun, J., Wood, E., Risk, B., Gundling, W.E., Jr., Kundaje, A., Gunawardena, H.P., Yu, Y., Xie, L., et al. (2012). Long noncoding RNAs are rarely translated in two human cell lines. Genome Res. *22*, 1646–1657.

10. Cesana, M., Cacchiarelli, D., Legnini, I., Santini, T., Sthandier, O., Chinappi, M., Tramontano, A., and Bozzoni, I. (2011). A long noncoding RNA controls muscle differentiation by functioning as a competing endogenous RNA. Cell *147*, 358–369.

11. Fatica, A., and Bozzoni, I. (2014). Long non-coding RNAs: new players in cell differentiation and development. Nat. Rev. Genet. *15*, 7–21.

12. Dey, B.K., Pfeifer, K., and Dutta, A. (2014). The H19 long noncoding RNA gives rise to microRNAs miR-675-3p and miR-675-5p to promote skeletal muscle differentiation and regeneration. Genes Dev. *28*, 491–501.

13. Chen, Y.A., and Aravin, A.A. (2015). Non-Coding RNAs in Transcriptional Regulation: The review for *Current Molecular Biology Reports*. Curr. Mol. Biol. Rep. *1*, 10–18.

14. Bonasio, R., and Shiekhattar, R. (2014). Regulation of transcription by long noncoding RNAs. Annu. Rev. Genet. *48*, 433–455.

15. Vance, K.W., and Ponting, C.P. (2014). Transcriptional regulatory functions of nuclear long noncoding RNAs. Trends Genet. *30*, 348–355.

16. Grote, P., and Herrmann, B.G. (2015). Long noncoding RNAs in organogenesis: making the difference. Trends Genet. *31*, 329–335.

17. Mathieu, E.-L., Belhocine, M., Dao, L.T., Puthier, D., and Spicuglia, S. (2014). [Functions of lncRNA in development and diseases]. Med. Sci. (Paris) *30*, 790–796.

18. Dey, B.K., Mueller, A.C., and Dutta, A. (2014). Long non-coding RNAs as emerging regulators of differentiation, development, and disease. Transcription *5*, e944014.

19. Tang, J.-Y., Lee, J.-C., Chang, Y.-T., Hou, M.-F., Huang, H.-W., Liaw, C.-C., and Chang, H.W. (2013). Long noncoding RNAs-related diseases, cancers, and drugs. Sci. World J. *2013*, 943539.

20. Ling, H., Vincent, K., Pichler, M., Fodde, R., Berindan-Neagoe, I., Slack, F.J., and Calin, G.A. (2015). Junk DNA and the long non-coding RNA twist in cancer genetics. Oncogene *34*, 5003–5011.

21. Liu, X.H., Sun, M., Nie, F.Q., Ge, Y.B., Zhang, E.B., Yin, D.D., Kong, R., Xia, R., Lu, K.H., Li, J.H., et al. (2014). Lnc RNA HOTAIR functions as a competing endogenous RNA to regulate HER2 expression by sponging miR-331-3p in gastric cancer. Mol. Cancer *13*, 92.

22. Quinn, J.J., and Chang, H.Y. (2016). Unique features of long non-coding RNA biogenesis and function. Nat. Rev. Genet. *17*, 47–62.

23. Caretti, G., Schiltz, R.L., Dilworth, F.J., Di Padova, M., Zhao, P., Ogryzko, V., Fuller-Pace, F.V., Hoffman, E.P., Tapscott, S.J., and Sartorelli, V. (2006). The RNA helicases p68/p72 and the noncoding RNA SRA are coregulators of MyoD and skeletal muscle differentiation. Dev. Cell *11*, 547–560.

24. Zhou, L., Sun, K., Zhao, Y., Zhang, S., Wang, X., Li, Y., Lu, L., Chen, X., Chen, F., Bao, X., et al. (2015). Linc-YY1 promotes myogenic differentiation and muscle regeneration through an interaction with the transcription factor YY1. Nat. Commun. *6*, 10026.

25. Li, Y., Chen, X., Sun, H., and Wang, H. (2018). Long non-coding RNAs in the regulation of skeletal myogenesis and diseases. Cancer Lett. *417*, 58–64.

26. Korostowski, L., Sedlak, N., and Engel, N. (2012). The Kcnq1ot1 long non-coding RNA affects chromatin conformation and expression of Kcnq1, but does not regulate its imprinting in the developing heart. PLoS Genet. *8*, e1002956.

27. Han, P., Li, W., Lin, C.-H., Yang, J., Shang, C., Nuernberg, S.T., Jin, K.K., Xu, W., Lin, C.Y., Lin, C.J., et al. (2014). A long noncoding RNA protects the heart from pathological hypertrophy. Nature *514*, 102–106.

28. Kallen, A.N., Zhou, X.-B., Xu, J., Qiao, C., Ma, J., Yan, L., Lu, L., Liu, C., Yi, J.S., Zhang, H., et al. (2013). The imprinted H19 lncRNA antagonizes let-7 microRNAs. Mol. Cell *52*, 101–112.

29. Wang, J., Gong, C., and Maquat, L.E. (2013). Control of myogenesis by rodent SINE-containing lncRNAs. Genes Dev. *27*, 793–804.

30. Wang, G.Q., Wang, Y., Xiong, Y., Chen, X.-C., Ma, M.L., Cai, R., Gao, Y., Sun, Y.M., Yang, G.S., and Pang, W.J. (2016). Sirt1 AS lncRNA interacts with its mRNA to inhibit muscle formation by attenuating function of miR-34a. Sci. Rep. *6*, 21865.

31. Anderson, D.M., Anderson, K.M., Chang, C.-L., Makarewich, C.A., Nelson, B.R., McAnally, J.R., Kasaragod, P., Shelton, J.M., Liou, J., Bassel-Duby, R., and Olson, E.N. (2015). A micropeptide encoded by a putative long noncoding RNA regulates muscle performance. Cell *160*, 595–606.

32. Nelson, B.R., Makarewich, C.A., Anderson, D.M., Winders, B.R., Troupes, C.D., Wu, F., Reese, A.L., McAnally, J.R., Chen, X., Kavalali, E.T., et al. (2016). A peptide encoded by a transcript annotated as long noncoding RNA enhances SERCA activity in muscle. Science *351*, 271–275.

33. He, H., and Liu, X. (2013). Characterization of transcriptional complexity during longissimus muscle development in bovines using high-throughput sequencing. PLoS ONE *8*, e64356.

34. Sun, J., Li, M., Li, Z., Xue, J., Lan, X., Zhang, C., Lei, C., and Chen, H. (2013). Identification and profiling of conserved and novel microRNAs from Chinese Qinchuan bovine longissimus thoracis. BMC Genomics *14*, 42.

35. Sun, X., Li, M., Sun, Y., Cai, H., Li, R., Wei, X., Lan, X., Huang, Y., Lei, C., and Chen, H. (2015). The developmental transcriptome landscape of bovine skeletal muscle defined by Ribo-Zero ribonucleic acid sequencing. J. Anim. Sci. *93*, 5648–5658.

36. Li, M., Sun, X., Cai, H., Sun, Y., Plath, M., Li, C., Lan, X., Lei, C., Lin, F., Bai, Y., and Chen, H. (2016). Long non-coding RNA ADNCR suppresses adipogenic differentiation by targeting miR-204. Biochim. Biophys. Acta *1859*, 871–882.

37. Chen, J.F., Mandel, E.M., Thomson, J.M., Wu, Q., Callis, T.E., Hammond, S.M., Conlon, F.L., and Wang, D.Z. (2006). The role of microRNA-1 and microRNA-133 in skeletal muscle proliferation and differentiation. Nat. Genet. *38*, 228–233.

38. Liu, N., Williams, A.H., Kim, Y., McAnally, J., Bezprozvannaya, S., Sutherland, L.B., Richardson, J.A., Bassel-Duby, R., and Olson, E.N. (2007). An intragenic MEF2-dependent enhancer directs muscle-specific expression of microRNAs 1 and 133. Proc. Natl. Acad. Sci. USA *104*, 20844–20849.

39. Li, H., Yang, J., Wei, X., Song, C., Dong, D., Huang, Y., Lan, X., Plath, M., Lei, C., Ma, Y., et al. (2017). CircFUT10 reduces proliferation and facilitates differentiation of myoblasts by sponging miR-133a. J. Cell. Physiol. *233*, 4643–4651.

40. Zhou, X., Zhang, W., Jin, M., Chen, J., Xu, W., and Kong, X. (2017). lncRNA MIAT functions as a competing endogenous RNA to upregulate DAPK2 by sponging miR-22-3p in diabetic cardiomyopathy. Cell Death Dis. *8*, e2929.

41. Yan, H., Rao, J., Yuan, J., Gao, L., Huang, W., Zhao, L., and Ren, J. (2017). Long non-coding RNA MEG3 functions as a competing endogenous RNA to regulate ischemic neuronal death by targeting miR-21/PDCD4 signaling pathway. Cell Death Dis. *8*, 3211.

42. Liu, H.Z., Wang, B.S., Zhang, J.J., Zhang, S.Z., Wang, Y.L., Zhang, J., Lv, C., and Song, X. (2017). A novel lnc-PCF promotes the proliferation of TGF-beta 1-activated epithelial cells by targeting miR-344a-5p to regulate map3k11 in pulmonary fibrosis. Cell Death Dis. *8*, e3137.

43. Zhuang, L.K., Yang, Y.T., Ma, X., Han, B., Wang, Z.S., Zhao, Q.Y., Wu, L.Q., and Qu, Z.Q. (2016). MicroRNA-92b promotes hepatocellular carcinoma progression by targeting Smad7 and is mediated by long non-coding RNA XIST. Cell Death Dis. *7*, e2203.

44. Li, H., Wei, X., Yang, J., Dong, D., Huang, Y., Lan, X., Plath, M., Lei, C., Qi, X., Bai, Y., and Chen, H. (2017). Developmental transcriptome profiling of bovine muscle tissue reveals an abundant GosB that regulates myoblast proliferation and apoptosis. Oncotarget *8*, 32083–32100.

45. Wei, X., Li, H., Yang, J., Hao, D., Dong, D., Huang, Y., Lan, X., Plath, M., Lei, C., Lin, F., et al. (2017). Circular RNA profiling reveals an abundant circLMO7 that regulates myoblasts differentiation and survival by sponging miR-378a-3p. Cell Death Dis. *8*, e3153.

46. Guttman, M., and Rinn, J.L. (2012). Modular regulatory principles of large non-coding RNAs. Nature *482*, 339–346.

47. Tuo, Y.L., Li, X.M., and Luo, J. (2015). Long noncoding RNA UCA1 modulates breast cancer cell growth and apoptosis through decreasing tumor suppressive miR-143. Eur. Rev. Med. Pharmacol. Sci. *19*, 3403–3411.

48. Liu, D., Li, Y., Luo, G., Xiao, X., Tao, D., Wu, X., Wang, M., Huang, C., Wang, L., Zeng, F., and Jiang, G. (2017). LncRNA SPRY4-IT1 sponges miR-101-3p to promote proliferation and metastasis of bladder cancer cells through up-regulating EZH2. Cancer Lett. *388*, 281–291.

OMTN, Volume *12*

Supplemental Information

Long Non-coding RNA Profiling Reveals an Abundant MDNCR that Promotes Differentiation of Myoblasts by Sponging miR-133a

Hui Li, Jiameng Yang, Rui Jiang, Xuefeng Wei, Chengchuang Song, Yongzhen Huang, Xianyong Lan, Chuzhao Lei, Yun Ma, Linyong Hu, and Hong Chen

Figure S1

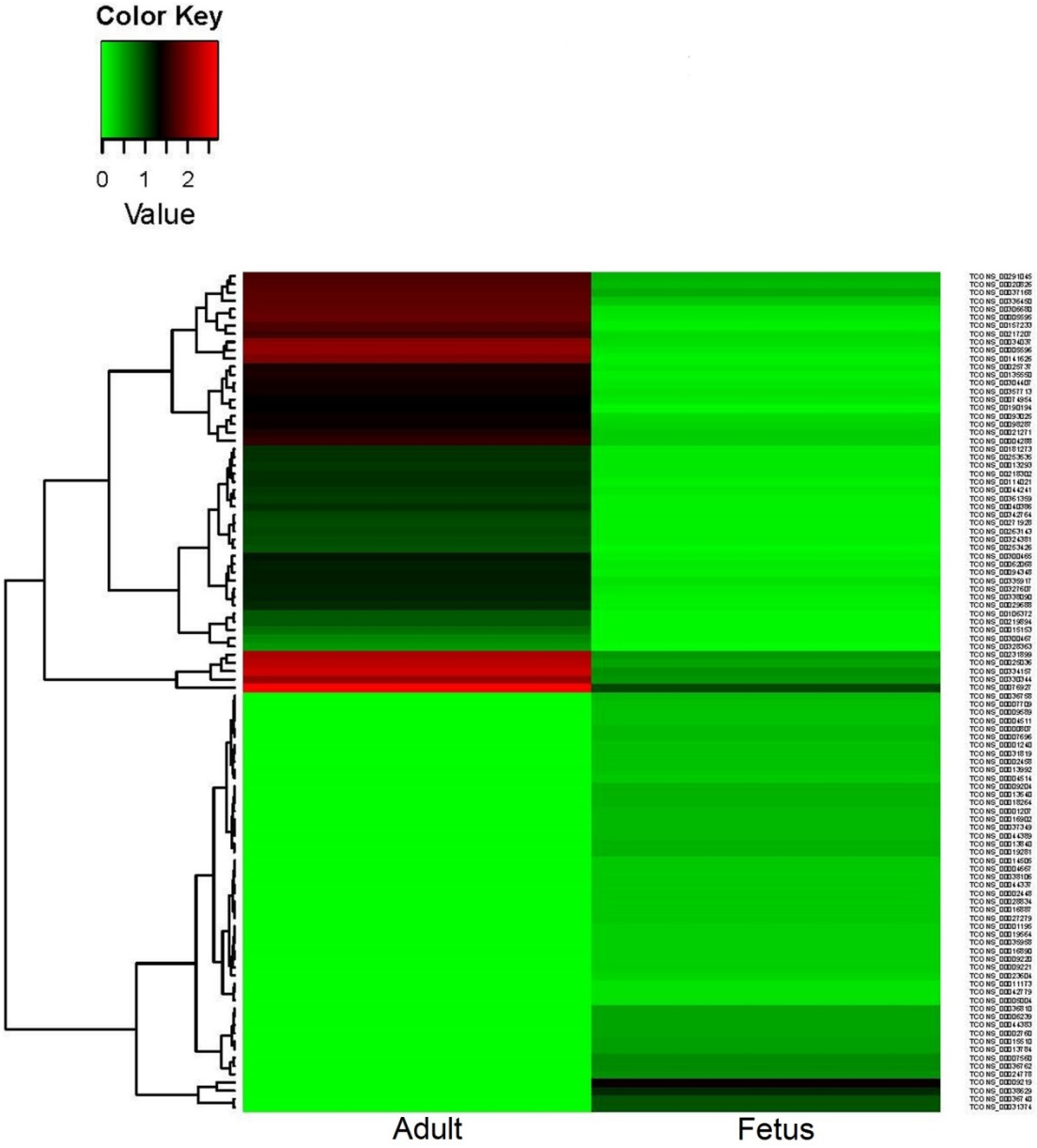

Figure S1. Clustered heat map showing abundances of randomly selected 100 differentially expressed lncRNAs.

Table S5a primers for qPCR

Name	Forward primer 5'→3'	Reverse primer 5'→3'
MDNCR	TCATGCCTGGGACTTGGAAC	GTGGGTCGTCCGTTCCTTTA
PCNA	TCCAGAACAAGAGTATAGC	TACAACAGCATCTCCAAT
CyclinD1	CCGTCCATGCGGAAGATC	CAGGAAGCGGTCCAGGTAG
β-actin	CATCCTGACCCTCAAGTA	CTCGTTGTAGAAGGTGTG
MyoG	CAAATCCACTCCCTGAAA	GCATAGGAAGAGATGAACA
MyhC	TGCTCATCTCACCAAGTTCC	CACTCTTCACTCTCATGGACC
MyoD	ACGGCATGATGGACTACAGC	AGGCAGTCGAGGCTCGACA
Bcl-2	ATGACCGAGTACCTGAAC	CATACAGCTCCACAAAGG
Bax	GAGATGAATTGGACAGTAACA	TTGAAGTTGCCGTCAGAA
Caspase-9	TGGTGGTCATCCTGTCTC	CATCCATCTGTGCCATAAAC
Caspase-3	CAGCGTCGTAGCTGAACGTA	CCAGAGTCCATTGATTTGCTTCC
bta-miR-133a	GTGCTTTGGTCCCCTTCAAC	GCAGGGTCCGAGGTATTC
U6	GCTTCGGCAGCACATATACTAAAAT	CGCTTCACGAATTTGCGTGTCAT

Table S5b primers for vector construction

Name	Primer sequence 5'→3'
pcDNA-MDNCR-F	CCCAAGCTTGCATTCATCCCGGTCAATTTT
pcDNA-MDNCR-R	GGGGTACCAGTTTATTGATGAGTCCAGGGCA
pCK-MDNCR-W-F	CCGCTCGAGGCATTCATCCCGGTCAATTTT
pCK-MDNCR-W-R	ATAAGAATGCGGCCGCAGTTTATTGATGAGTCCAGGGCA
pCK-GosB-3'UTR-W-F	CCGCTCGAG AGCTTTAGACAAAACAAACAAACAC
pCK-GosB-3'UTR-W-R	ATAAGAATGCGGCCGCTTTATTGGCGACAGTGCAGA
pCK-miR-133a 2×-F	GCTCGAGCAGCTGGTTGAAGGGGACCAAACAGCTGG TTGAAGGGGACCAAA
pCK-miR-133a 2×-R	GGCGGCCGCTTTGGTCCCCTTCAACCAGCTGTTTGGTC CCCTTCAACCAGCTG

Notes: The nucleotide with underline is the restriction enzyme cutting site.

Text S1. Sequence of cattle MDNCR.

lncRNA MDNCR

GCATTCATCCCGGTCAATTTTGGTTTCAGATCGTGGCGACTGGTGGACAGGGGTCTTGA
CAGAGGCTCGCCCTGGGGCTGGGGCAGCGGAGGCGTAGCTGGCAGCCGTGGGCAGGT
GAAGACAGCGCTCTGCCGGCCAGGTGAGTCCCCTTCTCCTCGCTGGTCCTTGCTCTCC
TGGTCTCCTGCAGAAGGAGGTTCTGGGGAGCGCGGGCCAGCGAGGTGGAGAGGCTG
GCCTCCCGGCAGAGCAGGACGCAGGCTGGTCAGGCAGCACAGGTGATATCGTCTCAG
GGGAGCTGAGACAGGGCGGGCTGGGGGCCGCGGGATGGGGTGCCGCGGGCTGCCCC
AGGTGGCAAGGGCATTTCCAGAGAGCCAGGCGGGAGCTTAGCAGGCAGGGCTGCCAG
CACGTGTAGGGGGCACTCAGGCCCCCGGGGCGAGCAGGACAGGGTGGGGACTCAGG
ACAGAGGGGTTCCCAGCCGCCACTTCACCCACTGTAATTCACTTAGTAGTAGGTCACA
GGAGCGGCTCCGGCCAGGCGTTCTCAGGCCTGAGCCAGAGCCTCGAGGGCCGGAGAA
TGAGAGAGAAGGCAGCGCAGTGCGCGGGCAACCGCGGCGGGATGTCATCTGGGGGG
CGGTGGCCGCGGGACAGGCCCGGAGAGATACCTGCAGCAGGGAGGCTGCGCGGGCCC
AGCCCGTGGACGCCAGCCCCACGCAGCACTGCGGCCCGGGAGCCACGCGGGAGGGC
CCCAGTGCACTTGGGGACACTGGGGACACTTGACCCGAACCGCTGGCCCTTGGGATG
GGCATGAGAGATAGAACAGCACCCAGGGGAGTCAAGGACACGGGCGAGACCAGGCT
AGGTGGGGCGGGTGGGGGGGCGTGAATGTGCACTCTCGGGGGAAGGGAGGCCAGGG
CACAGGCAGGGGCGAGGGGCCAGAGCCGGGCACCGAGCCAGTGGGAGGGGCATTGG
ACTTCGAGCTCGTGGCCAAGGCGGGCCTCTGCGGGCGATGACGGAGCGGGATCGGTG
CCTCTGAGCTCGGAACGGAGACGGAGCCACGTCTCCAGTGGGGTGTTGGTGCCTGCC
AGCCACGGAGGCCGGGCGGCCAGGACGCGCACAGAGGGATATGATATGGTCCGGTGT
GATGGAGAGAGCAGGCGGGACCGTCCAGCCTCCCAGGACACTGGCCCCGCGGGGAG
CCCGGATATCGACGTTCCTTTAGTCTCCTGACGGAGCAGACACACCACTGCTGCTCTTC
AGACACCCAGAACCCTCAAGATGACAAGAGATGGTGCTACCCAGCTCATGCCTGGGA
CTTGGAACACGGACTTCTTCAAGTCTTCTAGCTCTGACTCAAGAATATGCTGCATTTTG
GAACCACTACACACCCTAACTCAGGAATCAGCTCTGGAAGGTTGACCTAAAGGAACG
GACGACCCACACCACCGGAAGAGCAGCCCCCGCGGCGACACCCACCCCGGCCCGGC
GACTCCATCTCTGCGGCCCCCCCCTGCCTCAGCCCCGAGACCACCGACAGCCTCCCTC
CCTCCTTTTCCTCCTTTTCTGACTCTATTTTCTGATCTTCTCTCTGCTATCCTTTGCTCAG
GAGACTCAGAGCCTCCAGAGCCCCGTTCTCCCCGTCCCCCTTGAATCAATTTGCACTA
AAAGTCGTTTGCACTGGTTGGGGCTCTGGAGCCAGCCCTGGTCTCTGAGCGTGTGTAA
GCGCGCGTGTGTGCACACTGCTGAATGTGTAGGCCTCCTTGGCCCGTGCCCCCGCCCA
GCACCCTTCCCACACTTGCGGGTGCCTGGGAGGGGGCCCGAGTGGGGGGGCCCGCGT
GTGAGGGGCCCCGCCCGCCCGCACCGAGTCTGGAGGCTCCGAACATCAGGAGCACAC
ACCAAGCATGAACGTGTGTCCATCTTGCCTAGTGTCCCTCCCTGCCAGGGCCTCCTCAG
ATGCCCTGGACTCATCAATAAACTCAGT

Text S2. Cattle MDNCR sequence revealed the presence of thirty-two putative miR-133a binding sites.

Version: RNAhybrid 2.2
Command line:/vol/bioapps/bin/RNAhybrid.bin -n 22 -q /var/bibiserv2/anonymous/rnahybrid/29/09/40/bibiserv2_2017-07-29_094018_50b4M/rnahybrid_input_mirna_sequences.file -b 40 -m 1974 -s 3utr_human -t /var/bibiserv2/anonymous/rnahybrid/29/09/40/bibiserv2_2017-07-29_094018_50b4M/rnahybrid_input_target_rna_sequences_.file
searching
dataset: 1
mde of bta-miR-133a: -49.200005
Individual hits
---

dataset: 1
target: TCONS_00238678
length: 1973
miRNA : bta-miR-133a
length: 22

mfe: -31.6 kcal/mol
p-value: 1.000000e+00

position 1789
```
target 5'  U  G   GCCUG          C  G 3'
            GC GGU     GGAGGGGGCC GA
            CG CCA     CUUCCCCUGG UU
miRNA  3' GU  A   A              U    5'
```

---

dataset: 1
target: TCONS_00238678
length: 1973
miRNA : bta-miR-133a
length: 22

mfe: -30.0 kcal/mol
p-value: 1.000000e+00

position 890
```
target 5'      C  GG       A        G 3'
```

```
               GG  GAAGGG GGCCAGG
               CC  CUUCCC CUGGUUU
miRNA  3’ GUCGA  AA                5’
```

---

dataset: 1
target: TCONS_00238678
length: 1973
miRNA : bta-miR-133a
length: 22

mfe: -28.8 kcal/mol
p-value: 1.000000e+00

position 913

```
target 5’ A   A  GGC            G 3’
           GGC GG   GAGGGG CCAGA
           UCG CC   UUCCCC GGUUU
miRNA  3’ G   A  AAC      U       5’
```

---

dataset: 1
target: TCONS_00238678
length: 1973
miRNA : bta-miR-133a
length: 22

mfe: -28.6 kcal/mol
p-value: 1.000000e+00

position 305

```
target 5’ G      GGGCCGCG   U    U    C  3’
           GGCUGG         GGA GGGG GCCG
           UCGACC         CUU CCCC UGGU
miRNA  3’ G      AA                  UU 5’
```

---

dataset: 1
target: TCONS_00238678
length: 1973
miRNA : bta-miR-133a

length: 22

mfe: -28.6 kcal/mol
p-value: 1.000000e+00

position 859
```
target 5’ G   G             GU  A 3’
           GGC GGU  GGGGGGGC  GA
           UCG CCA  UUCCCCUG  UU
miRNA  3’ G   A   AC        GU    5’
```

---

dataset: 1
target: TCONS_00238678
length: 1973
miRNA : bta-miR-133a
length: 22

mfe: -28.0 kcal/mol
p-value: 1.000000e+00

position 253
```
target 5’ A       CAGGCAGCACAGG   UAUCGUCUC      G     A 3’
           GGCUGGU              UGA          AGGGGA CUGAG
           UCGACCA              ACU          UCCCCU GGUUU
miRNA  3’ G                                             5’
```

---

dataset: 1
target: TCONS_00238678
length: 1973
miRNA : bta-miR-133a
length: 22

mfe: -26.5 kcal/mol
p-value: 1.000000e+00

position 432
```
target 5’ G   A  ACAG GU      U    A 3’
           AGC GG    G  GGGGAC CAGG
           UCG CC    C  CCCCUG GUUU
miRNA  3’ G   A  AA   UU             5’
```

---

dataset: 1
target: TCONS_00238678
length: 1973
miRNA : bta-miR-133a
length: 22

mfe: -26.4 kcal/mol
p-value: 1.000000e+00

position 188
```
target 5’ A  GA    CUGG    C C       C 3’
           AG  GGUU    GGAG G GGGCCAG
           UC  CCAA    CUUC C CCUGGUU
miRNA  3’ G  GA                     U 5’
```

---

dataset: 1
target: TCONS_00238678
length: 1973
miRNA : bta-miR-133a
length: 22

mfe: -26.3 kcal/mol
p-value: 1.000000e+00

position 605
```
target 5’ G    G  A  UCAUCU       G U  3’
           CGGC GG UG      GGGGGGC G
           GUCG CC AC      UCCCCUG U
miRNA  3’       A  A  U            G UU 5’
```

---

dataset: 1
target: TCONS_00238678
length: 1973
miRNA : bta-miR-133a
length: 22

mfe: -26.2 kcal/mol

p-value: 1.000000e+00

position 1077

```
target 5’ C    CAC  AG CC   C       A 3’
           CAGC   GG  G  GGG GGCCAGG
           GUCG   CC  C  CCC CUGGUUU
miRNA  3’       A    AA UU            5’
```

---

dataset: 1
target: TCONS_00238678
length: 1973
miRNA : bta-miR-133a
length: 22

mfe: -26.2 kcal/mol
p-value: 1.000000e+00

position 1669

```
target 5’   A       GG CUCU   G    C 3’
             CUGGUUG  G    GGA CCAG
             GACCAAC  C    CCU GGUU
miRNA  3’ GUC       UU C           U 5’
```

---

dataset: 1
target: TCONS_00238678
length: 1973
miRNA : bta-miR-133a
length: 22

mfe: -25.7 kcal/mol
p-value: 1.000000e+00

position 391

```
target 5’ G     CCAGCACG  U       A    3’
           GGCUG         UG AGGGGGC
           UCGAC         AC UCCCCUG
miRNA  3’ G     CA         U       GUUU 5’
```

---

dataset: 1
target: TCONS_00238678
length: 1973
miRNA : bta-miR-133a
length: 22

mfe: -24.5 kcal/mol
p-value: 1.000000e+00

position 971
```
target 5’ G    C  GGCC    C     U   3’
           AGCU GU    AAGG GGGCC
           UCGA CA    UUCC CCUGG
miRNA  3’ G    C  AC            UUU 5’
```

---

dataset: 1
target: TCONS_00238678
length: 1973
miRNA : bta-miR-133a
length: 22

mfe: -24.3 kcal/mol
p-value: 1.000000e+00

position 37
```
target 5’  C A     G  C     UCUUGA    G 3’
            G CUGGU GA AGGGG      CAGA
            C GACCA CU UCCCC      GUUU
miRNA  3’ GU       A        UG          5’
```

---

dataset: 1
target: TCONS_00238678
length: 1973
miRNA : bta-miR-133a
length: 22

mfe: -24.3 kcal/mol
p-value: 1.000000e+00

position 996

```
target 5’ G     GAUGAC     C         U 3’
           CGGC       GGAG GGGAUCGG
           GUCG       CUUC CCCUGGUU
miRNA  3’       ACCAA               U 5’
```

---

dataset: 1
target: TCONS_00238678
length: 1973
miRNA : bta-miR-133a
length: 22

mfe: -24.1 kcal/mol
p-value: 1.000000e+00

position 1394

```
target 5’ U      CUGGAA       CCUAA    AAC     G     3’
           CAGCU       GGUUGA      AGG    GGAC
           GUCGA       CCAACU      UCC    CCUG
miRNA  3’                                    GUUU 5’
```

---

dataset: 1
target: TCONS_00238678
length: 1973
miRNA : bta-miR-133a
length: 22

mfe: -23.8 kcal/mol
p-value: 1.000000e+00

position 75

```
target 5’ G       GGCAGC      CGUAGCU  CA     U  3’
           GGCUGG       GGAGG        GG  GCCG
           UCGACC       CUUCC        CC  UGGU
miRNA  3’ G       AA                          UU 5’
```

---

dataset: 1
target: TCONS_00238678
length: 1973

miRNA : bta-miR-133a
length: 22

mfe: -23.8 kcal/mol
p-value: 1.000000e+00

position 1125
```
target 5’ U   CC   GUGA     AGAGCAGGC       U  3’
           GGU  GGU    UGGAG          GGGACCG
           UCG  CCA    ACUUC          CCCUGGU
miRNA  3’ G   A                              UU 5’
```

---

dataset: 1
target: TCONS_00238678
length: 1973
miRNA : bta-miR-133a
length: 22

mfe: -23.2 kcal/mol
p-value: 1.000000e+00

position 342
```
target 5’ C   G   C       CAUUU     G 3’
           CAG UGG   AAGGG     CCAGA
           GUC ACC   UUCCC     GGUUU
miRNA  3’      G   AAC     CU          5’
```

---

dataset: 1
target: TCONS_00238678
length: 1973
miRNA : bta-miR-133a
length: 22

mfe: -23.1 kcal/mol
p-value: 1.000000e+00

position 742
```
target 5’ C    GCACU   GGACACU      A    3’
           CAGU     UGG        GGGGAC
           GUCG     ACC        CCCCUG
```

```
miRNA  3’                AACUU         GUUU 5’
```

---

dataset: 1
target: TCONS_00238678
length: 1973
miRNA : bta-miR-133a
length: 22

mfe: -22.9 kcal/mol
p-value: 1.000000e+00

position 1814

```
target 5’          G  GG     C    C  3’
                    UG  GGGG CCG
                    AC  CCCC GGU
miRNA  3’ GUCGACCA  UU     U    UU 5’
```

---

dataset: 1
target: TCONS_00238678
length: 1973
miRNA : bta-miR-133a
length: 22

mfe: -22.8 kcal/mol
p-value: 1.000000e+00

position 944

```
target 5’ G   CA  G        C       C 3’
           AGC  GU GGAGGGG AUUGGA
           UCG  CA CUUCCCC UGGUUU
miRNA  3’ G   AC  A                5’
```

---

dataset: 1
target: TCONS_00238678
length: 1973
miRNA : bta-miR-133a
length: 22

mfe: -22.2 kcal/mol
p-value: 1.000000e+00

position 1173
```
target 5’ A       CCCCGC     GC     U 3’
           CA CUGG      GGGGA  CCGGA
           GU GACC      CCCCU  GGUUU
miRNA  3’    C    AACUU              5’
```

---

dataset: 1
target: TCONS_00238678
length: 1973
miRNA : bta-miR-133a
length: 22

mfe: -22.1 kcal/mol
p-value: 1.000000e+00

position 661
```
target 5’ G    A  GA  CUGC C   C    C 3’
           CAGC GG  GG    G GGG CCAG
           GUCG CC  CU    C CCC GGUU
miRNA  3’       A  AA  U        U    U 5’
```

---

dataset: 1
target: TCONS_00238678
length: 1973
miRNA : bta-miR-133a
length: 22

mfe: -21.9 kcal/mol
p-value: 1.000000e+00

position 502
```
target 5’ G    A   CACA    C  CUCC      G 3’
           UAGU GGU    GGAG GG    GGCCAG
           GUCG CCA    CUUC CC    CUGGUU
miRNA  3’       A   A                  U 5’
```

---

dataset: 1
target: TCONS_00238678
length: 1973
miRNA : bta-miR-133a
length: 22

mfe: -21.9 kcal/mol
p-value: 1.000000e+00

position 813
```
target 5’ A    ACCCAG  GAGUCAAG  CAC   C A      G 3’
           CAGC       GG         GA   GGG G GACCAG
           GUCG       CC         CU   UCC C CUGGUU
miRNA  3’       A        AA                       U 5’
```

---

dataset: 1
target: TCONS_00238678
length: 1973
miRNA : bta-miR-133a
length: 22

mfe: -21.5 kcal/mol
p-value: 1.000000e+00

position 781
```
target 5’  C     CCCUU      G  C 3’
            GCUGG      GGGAU GG
            CGACC      CCCUG UU
miRNA  3’ GU     AACUUC     G  U 5’
```

---

dataset: 1
target: TCONS_00238678
length: 1973
miRNA : bta-miR-133a
length: 22

mfe: -21.4 kcal/mol
p-value: 1.000000e+00

position 1825
```
target 5’  N  GUG        CC   C  3’
            GC    UGAGGGG  CCG
            CG    ACUUCCC  GGU
miRNA  3’ GU  ACCA       CU   UU 5’
```

---

dataset: 1
target: TCONS_00238678
length: 1973
miRNA : bta-miR-133a
length: 22

mfe: -21.1 kcal/mol
p-value: 1.000000e+00

position 1027
```
target 5’ G    C  AAC    AC  A    C  3’
           AGCU GG   GGAG  GG GCCA
           UCGA CC   CUUC  CC UGGU
miRNA  3’ G       AA         C    UU 5’
```

---

dataset: 1
target: TCONS_00238678
length: 1973
miRNA : bta-miR-133a
length: 22

mfe: -20.7 kcal/mol
p-value: 1.000000e+00

position 213
```
target 5’  N  GA        A  CU    U   3’
            GC  GGU GGAG GG  GGCC
            CG  CCA CUUC CC  CUGG
miRNA  3’ GU  A    A             UUU 5’
```

---

dataset: 1
target: TCONS_00238678

length: 1973
miRNA : bta-miR-133a
length: 22

mfe: -20.6 kcal/mol
p-value: 1.000000e+00

position 109

```
target 5’ G   A        ACAGCGCUCUGCC       U 3’
           GGC GGU GAAG              GGCCAGG
           UCG CCA CUUC              CUGGUUU
miRNA  3’ G   A   A    CC                    5’
```

---

dataset: 1
target: TCONS_00238678
length: 1973
miRNA : bta-miR-133a
length: 22

mfe: -20.2 kcal/mol
p-value: 1.000000e+00

position 1291

```
target 5’ C     CA   CCU      U   3’
           CAGCU   UG   GGGACU
           GUCGA   AC   CCCUGG
miRNA  3’       CCA  UUC      UUU 5’
```

Text S3. Cattle GosB gene 3'UTR revealed the presence of eighteen putative miR-133a binding sites.

Version: RNAhybrid 2.2
Command line:/vol/bioapps/bin/RNAhybrid.bin -n 22 -q /var/bibiserv2/anonymous/rnahybrid/08/08/21/bibiserv2_2018-01-08_082157_fRwfX/rnahybrid_input_mirna_sequences.file -D -b 30 -m 2200 -t /var/bibiserv2/anonymous/rnahybrid/08/08/21/bibiserv2_2018-01-08_082157_fRwfX/rnahybrid_input_target_rna_sequences_.file
searching
dataset: 1
mde of bta-miR-133a: -49.200005
Individual hits
---

dataset: 1
target: GosB 3'UTR
length: 2200
miRNA : bta-miR-133a
length: 22

mfe: -30.9 kcal/mol
p-value: undefined

position 209
```
target 5' G          CUUU      A    G 3'
           AGCUGG UGA    GGGGGC CGGG
           UCGACC ACU    CCCCUG GUUU
miRNA  3' G      A   U                5'
```

---

dataset: 1
target: GosB 3'UTR
length: 2200
miRNA : bta-miR-133a
length: 22

mfe: -28.5 kcal/mol
p-value: undefined

position 344
```
target 5' G      AGG   C    UG U   3'
```

```
           GGCUGG   GAG GGGG  U
           UCGACC   CUU CCCC  G
miRNA  3' G       AA          UG UUU 5'
```

---

dataset: 1
target: GosB 3'UTR
length: 2200
miRNA : bta-miR-133a
length: 22

mfe: -28.5 kcal/mol
p-value: undefined

position 880

```
target 5' G      CCGGAUUG  GG   A      U 3'
           AGUUGG         UG  GGG GCCGGG
           UCGACC         AC  CCC UGGUUU
miRNA  3' G       A          UU   C        5'
```

---

dataset: 1
target: GosB 3'UTR
length: 2200
miRNA : bta-miR-133a
length: 22

mfe: -27.8 kcal/mol
p-value: undefined

position 1892

```
target 5' C    CGUCUUCUGACUC   GUU  UU       U   3'
           CAGC             UGG   UG  GGGGACC
           GUCG             ACC   AC  CCCCUGG
miRNA  3'                       A    UU       UUU 5'
```

---

dataset: 1
target: GosB 3'UTR
length: 2200
miRNA : bta-miR-133a

length: 22

mfe: -27.4 kcal/mol
p-value: undefined

position 307
```
target 5’ G  A   GG GU      G   G 3’
          GG UGG  G  GGGGGC GGA
          UC ACC  C  CCCCUG UUU
miRNA  3’ G  G   AA UU      G     5’
```

---

dataset: 1
target: GosB 3’UTR
length: 2200
miRNA : bta-miR-133a
length: 22

mfe: -27.0 kcal/mol
p-value: undefined

position 232
```
target 5’      N   GG         G  C 3’
               GGU  GGAGGGGAU GA
               CCA  CUUCCCCUG UU
miRNA  3’ GUCGA   A          G  U 5’
```

---

dataset: 1
target: GosB 3’UTR
length: 2200
miRNA : bta-miR-133a
length: 22

mfe: -26.6 kcal/mol
p-value: undefined

position 1198
```
target 5’ G   AAC  GA  UUGCC       C   3’
          AGC   GG  GA     AGGGGGCC
          UCG   CC  CU     UCCCCUGG
miRNA  3’ G   A    AA              UUU 5’
```

---

dataset: 1
target: GosB 3’UTR
length: 2200
miRNA : bta-miR-133a
length: 22

mfe: -26.1 kcal/mol
p-value: undefined

position 2124
```
target 5’ G       C   CACU       C  3’
           GGCUGG UGG    GGGCCG
           UCGACC ACU    CCUGGU
miRNA  3’ G       A   UCC        UU 5’
```

---

dataset: 1
target: GosB 3’UTR
length: 2200
miRNA : bta-miR-133a
length: 22

mfe: -25.9 kcal/mol
p-value: undefined

position 372
```
target 5’ G          GG U         G 3’
           GGCUG  UG  G GGGCUGGA
           UCGAC  AC  C CCUGGUUU
miRNA  3’ G     CA  UU C           5’
```

---

dataset: 1
target: GosB 3’UTR
length: 2200
miRNA : bta-miR-133a
length: 22

mfe: -24.9 kcal/mol

p-value: undefined

position 64
```
target 5’   A    AG  GAG      AGAGA    G 3’
             CUGG  GA   AGGGGA     CAAA
             GACC  CU   UCCCCU     GUUU
miRNA  3’ GUC    AA           G          5’
```

---

dataset: 1
target: GosB 3’UTR
length: 2200
miRNA : bta-miR-133a
length: 22

mfe: -23.3 kcal/mol
p-value: undefined

position 805
```
target 5’  U     GCCUCUC   UUCAGGCAGC       G    3’
            GUUGG        UGA           AGGGGGC
            CGACC        ACU           UCCCCUG
miRNA  3’ GU     A                           GUUU 5’
```

---

dataset: 1
target: GosB 3’UTR
length: 2200
miRNA : bta-miR-133a
length: 22

mfe: -23.2 kcal/mol
p-value: undefined

position 2009
```
target 5’ A           CA     U   3’
           GGCUG  UGAG  GGGCC
           UCGAC  ACUU  CCUGG
miRNA  3’ G     CA    CC     UUU 5’
```

---

dataset: 1
target: GosB 3’UTR
length: 2200
miRNA : bta-miR-133a
length: 22

mfe: -22.1 kcal/mol
p-value: undefined

position 1006
```
target 5’ G    A ACUC       UGA    A 3’
           AGUU G    GAGGGGG   CAGA
           UCGA C    CUUCCCC   GUUU
miRNA  3’ G    C AA         UG       5’
```

---

dataset: 1
target: GosB 3’UTR
length: 2200
miRNA : bta-miR-133a
length: 22

mfe: -21.7 kcal/mol
p-value: undefined

position 1287
```
target 5’ U  A    CAAACUCC         GG U 3’
           GG CUGG        AAGGGG CU  G
           UC GACC        UUCCCC GG  U
miRNA  3’ G       AAC           U  UU   5’
```

---

dataset: 1
target: GosB 3’UTR
length: 2200
miRNA : bta-miR-133a
length: 22

mfe: -21.6 kcal/mol
p-value: undefined

position 136

```
target 5’  C    CCAUCG  C   A     U   3’
            GCUG       GA AGG GGACU
            CGAC       CU UCC CCUGG
miRNA  3’ GU    CAA               UUU 5’
```

---

dataset: 1
target: GosB 3’UTR
length: 2200
miRNA : bta-miR-133a
length: 22

mfe: -21.2 kcal/mol
p-value: undefined

position 1781

```
target 5’   U       UUUUCU     U  3’
             CUGGUUG       GGCCA
             GACCAAC       CUGGU
miRNA  3’ GUC        UUCCC       UU 5’
```

---

dataset: 1
target: GosB 3’UTR
length: 2200
miRNA : bta-miR-133a
length: 22

mfe: -20.5 kcal/mol
p-value: undefined

position 474

```
target 5’ A         CUCCCU     C  3’
           GGCUGGUU        GCCG
           UCGACCAA        UGGU
miRNA  3’ G         CUUCCCC    UU 5’
```

---

dataset: 1
target: GosB 3’UTR
length: 2200

miRNA : bta-miR-133a
length: 22

mfe: -20.3 kcal/mol
p-value: undefined

position 269

```
target 5’  U    CC  U   CCGUUUCACUU     C   3’
            GCUG  UG GGG           GGACC
            CGAC  AC UCC           CCUGG
miRNA  3’ GU    CA  U                  UUU 5’
```
